⊕Thieme

Homoadamantane and Adamantane Acylphloroglucinols from *Hypericum hirsutum*#

Authors
Julianna Max, Jörg Heilmann

Affiliation
Chair of Pharmaceutical Biology, University of Regensburg, Faculty of Chemistry and Pharmacy, Regensburg, Germany

Correspondence
Prof. Dr. Jörg Heilmann
Chair of Pharmaceutical Biology, University of Regensburg,
Faculty of Chemistry and Pharmacy
Universitätsstr. 31, 93053 Regensburg, Germany
Phone: + 49 94 19 43 47 59, Fax: + 49 94 19 43 49 90
joerg.heilmann@chemie.uni-regensburg.de

⊕ Supplementary material is available under
https://doi.org/10.1055/a-1617-7573

ABSTRACT

^{1}H NMR-guided fractionation of the petroleum ether extract of the aerial parts from *Hypericum hirsutum* yielded to the isolation of 19 polyprenylated polycyclic acylphloroglucinols. Structure elucidation based on 1D and 2D NMR spectroscopy together with high-resolution electrospray ionization mass spectroscopy revealed 14 acylphloroglucinols with a homoadamantane scaffold (**1–14**), while 5 further compounds showed an adamantane skeleton (**15–19**). Except for hookerione C (**15**), all isolated metabolites are hitherto unknown. While structurally-related metabolites have been isolated from other *Hypericum* species, it is the first report of admantan and homoadamantan type acylphloroglucinols in section *Taeniocarpium* Jaub. & Spach (Hypericaceae). The isolated compounds have been tested in a crystal violet-based *in vitro* assay on their properties to reduce the proliferation of human microvascular endothelial cells compared to hyperforin as the positive control. They showed a moderate reduction of proliferation with IC_{50} values in the range ~ 3–22 μM, with the homoadamantane-based compounds **2** and **4** being the most active. In addition, inhibition of the TNF-α-induced ICAM-1 expression was determined for **1–5, 7,** and **10–12**. Substances **3** and **12** reduced the ICAM-1 expression significantly (to 46.7 % of control for **3**, 62.3 % for **12,** at 50 μM).

Introduction

The family Hypericaceae includes 9 genera with approximately 540 species [1], of which nearly 500 belong to the genus *Hypericum* [2]. The high number and diversity of the species required a further classification of the genus into 36 sections by a combination of morphological, geographic, and phylogenetic aspects [2].

Within the Hypericaceae, acylphloroglucinols are a widespread class of secondary metabolites [3]. Based on diverse substitution patterns of the acylphloroglucinol core with prenyl and geranyl moieties followed by cyclizations and oxidations, this class of metabolites showed high structural diversity and is a valuable source of pharmacologically active compounds [4–10]. The formation of monocyclic [8], bicyclic [11], tricyclic [12], and complex caged representatives with an adamantane [13] or homoadamantane

[14] core has been described. In addition, the biosynthesis of heterocyclic [15, 16] and spiro [17] acylphloroglucinols has been reported.

Hypericum hirsutum ʟ. is a perennial herb with hirsute green parts resident to Northern Africa, Europe, and temperate Asia [18]. The chemical composition of the plant, especially the profile of prenylated acylphloroglucinols except for hyperforin and adhyperforin [19], is unknown. *H. hirsutum* is one of 28 species in section 18 *Taeniocarpium* Jaub. & Spach [18]. Two monocyclic acylphloroglucinol derivatives, 3-geranyl-1-(2-methylpropanoyl)phloroglucinol and 3-geranyl-1-(2-methylbutanoyl)phloroglucinol have been isolated from *H. linarioides* Bosse [20], but until

---

Dedicated to Prof. Dr. Otto Sticher on the occasion of his 85th birthday.
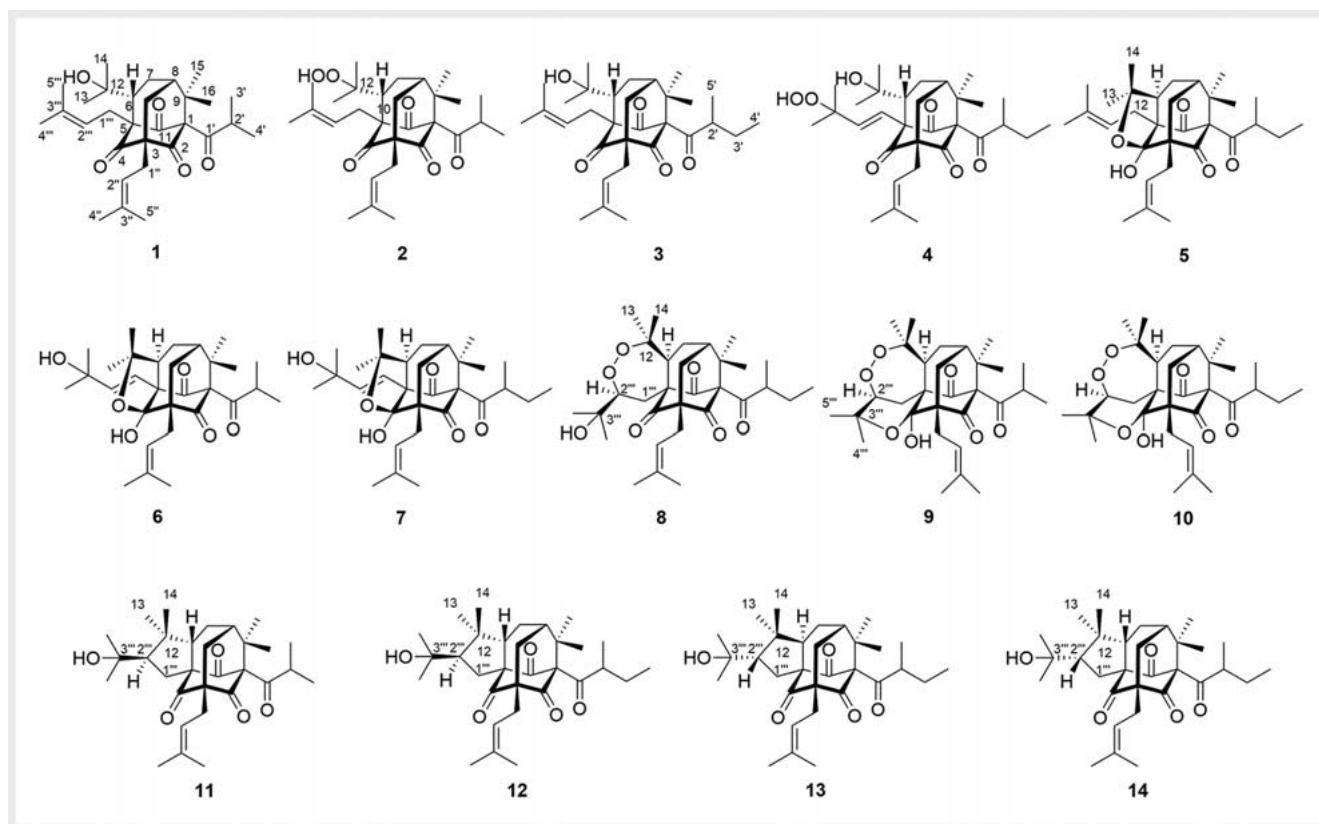
**► Fig. 1** Isolated homoadamantane-type acylphloroglucinols **1–14**.
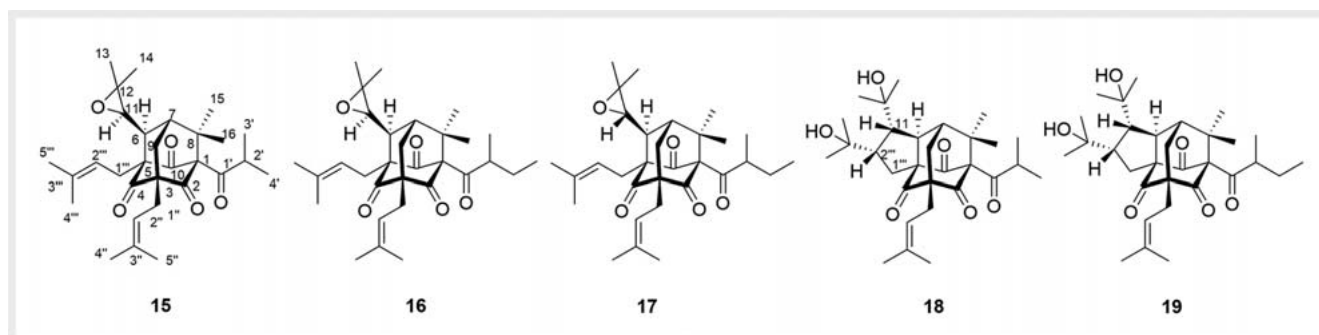
► Fig. 2 Isolated adamantane-type acylphloroglucinols **15–19**

now, most of the species from this section have not been investigated.

The present work deals with the isolation and structure elucidation of 19 acylphloroglucinols from *H. hirsutum* L, with 18 being hitherto undescribed. Antiproliferative activity was tested in an *in vitro* assay on an endothelial cell line (HMEC) to evaluate pharmacological *in vitro* effects. Furthermore, several compounds were investigated concerning their anti-inflammatory effects mediated by the reduction of the TNF-*α* induced ICAM-1 expression in endothelial cells. Two compounds with significant activity in the ICAM-1 assay were also tested in the Griess-Assay to determine their inhibition of nitric oxide production in LPS-activated macrophages.

Results and Discussion

From the petroleum ether (PE) extract of the aerial parts of *H. hirsutum* L. 18 new and 1 known polyprenylated polycyclic acylphloroglucinols (PPAPs) with homoadamantane (► **Fig. 1**) or adamantane (► **Fig. 2**) skeleton were isolated by a combination of Diaion HP-20 column chromatography, silica gel flash chromatography, centrifugal partition chromatography, and semi-preparative RP-18 HPLC. All fractions obtained from silica flash chromatography were analyzed with ^{1}H NMR to detect diagnostic triplet signals δ_H ~ 4.5–5.2 ppm of olefinic H-2 in prenyl groups or down-
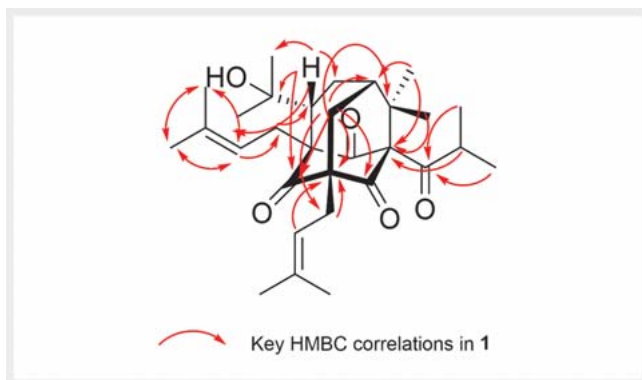
► **Fig. 3** Key HMBC correlations of **1**.

field shifted singlets ($\delta_H > 10$ ppm) corresponding to hydrogen-bonded hydroxyl groups.

The molecular formulas were determined by high-resolution electrospray ionization mass spectroscopy (ESI-HRMS), and the structures were elucidated by extensive 1D and 2D NMR spectroscopy. Substances **1–14** possess a tricyclo[4.3.1.1^{3,8}]undecane skeleton, also known as homoadamantane, whereas **15–19** exhibit a tricyclo[3.3.1.1^{3,7}]decane backbone trivially known as adamantane. Both rigid and caged ring systems themselves determine the relative configurations at the chiral centers C-1, C-3, C-5, and C-8 (homoadamantane) or C-1, C-3, C-5, and C-7 (adamantane). A general structure elucidation strategy of a PPAP with prenylated adamantane and homoadamantane core using 1D and 2D NMR is given in the Supporting Information.

Compound **1** was obtained as a colorless oil. The positive-ion ESI-HRMS gave a pseudomolecular ion at m/z 485.3266 [M + H]$^+$ corresponding to the molecular formula $C_{30}H_{44}O_5$. Besides the typical ^{1}H and ^{13}C NMR signals and HMBC correlations of a homoadamantane (► **Fig. 3** and **Fig. 1S**, Supporting Information), 2 additional sets of signals indicate that prenyl substituents were present. Thus, ^{1}H and ^{13}C NMR data (► **Table 1**) showed the presence of 2 olefinic protons H-2″/H-2‴ (δ_H 5.21/4.51) and olefinic carbons C-2″/C-2‴ (δ_C 119.0/119.9) and C-3″/C-3‴ (δ_C 135.2/136.7). HMBC experiments yielded H-C long-range correlations as follows: olefinic proton H-2‴ (δ_H 4.51) to C-1‴ (δ_C 34.1) and the geminal methyl groups C-4‴ (δ_C 18.1) and C-5‴ (δ_H 25.7); geminal methyl groups H/C-4‴ and H/C-5‴ vice versa and the olefinic carbons C-2‴ and C-3‴; H-1‴ (δ_H 3.19) to nonprotonated carbons C-4 (δ_C 208.2), C-5 (δ_C 70.9), C-11 (δ_C 206.2), C-3‴ and methine carbons C-6 (δ_C 49.4) and C-2″ (► **Fig. 3**; **Fig. 6S**, Supporting Information). These indicated one of the prenyl substituents at C-5. The second prenyl substituent is located at C-3 due to HMBC correlations from H-2″ to C-3 and H$_2$-10 to C-2″. Furthermore, an oxygen-bearing nonprotonated carbon (C-12, δ_C 75.9) linked to the geminal methyl groups C-13 (δ_C 26.8) and C-14 (δ_C 33.0) could be ascertained. HMBC correlations of H-6 (δ_H 1.83) and H$_2$-7 (δ_H 1.90/1.84) to the 2-hydroxyisopropyl side chain secured the linkage at C-6. The NOESY spectrum showed a correlation between H$_3$-16 (δ_H 1.25) and H-10a (δ_H 2.51), thereby allowing the respective assignment of methyl groups H$_3$-16 and H$_3$-15.

Because of the very similar chemical shifts of the hydrogen atoms nearby the remaining fifth chiral center C-6 (H-6: δ_H 1.83, H$_2$-7: δ_H 1.90/1.84, H-8: δ_H 1.89, H$_2$-10: δ_H 2.51/1.79), its relative stereochemistry is hard to determine. If H-6 is positioned on the same face as H-10b (δ_H 1.79) and thus β-oriented, as in otogirinin C from *H. erectum* Thunb. [21] and *H. sampsonii* Hance [22], there should be a NOE correlation between them, but their chemical shifts were too close to draw an unambiguous conclusion. If H-6 is α-oriented, a NOESY cross peak between H-6 and H$_3$-15 (δ_H 1.25) should be detected, similarly to pseudohenones F & G, isolated from *H. pseudohenryi* N. Robsen [23]. Nevertheless, the very similar shifts of H$_b$-7 (δ_H 1.84) and H-6 (δ_H 1.83) did not allow an unambiguous assignment of their NOE correlations. Due to weak NOESY cross-peaks of the geminal methyl groups H$_3$-13 (δ_H 1.40) and H$_3$-14 (δ_H 1.34) to H$_3$-15 (δ_H 1.25), an α-orientation of the 2-hydroxyisopropyl moiety and β orientation of H-6 was assumed (**Fig. 7S** and **8S**, Supporting Information). Furthermore, β orientation of H-6 in **1** is supported by an analogous conclusion from unambiguous NOEs of deshielded H-6 in **2**. Hence, compound **1** was assigned as a hitherto unknown homoadamantane acylphloroglucinol derivative and trivially named hirsutofolin A. A similar substance with aromatic acyl moiety was already isolated from *Clusia obdeltifolia* Bittrich (Clusiaceae) [24].

Compound **2** was isolated as a colorless oil and displayed a positive ESI-HRMS pseudomolecular ion at m/z 501.3220 [M + H]$^+$, consistent with a molecular formula of $C_{30}H_{44}O_6$. ^{1}H and ^{13}C NMR spectra matched those of **1** well except for 4 positions (► **Table 1**). There was a significantly deshielded nonprotonated carbon (C-12, δ_C 87.3 compared to δ_C 75.9 in **1**) as well as a high field shift of the methine carbon C-6 (δ_C 43.4) and geminal methyl groups C-13 (δ_C 21.7) and C-14 (δ_C 26.7). These chemical shifts, an extra oxygen atom in the molecular formula, and identical 2D NMR correlations with **1** supported the assumption that a peroxide replaced the hydroxyl group. Such an influence of replacing a hydroxyl with a peroxy group has also been reported for the 2 corresponding compounds, peroxysampsone A and plukenetione C [25]. The deshielded H-6 (δ_H 2.38, instead of 1.83 in **1**) showed unambiguous NOE correlations to neighbored hydrogen atoms. Cross peaks of H-10a (δ_H 2.53) and H$_3$-16 (δ_H 1.25), H-10b (δ_H 1.84) and H-6 (δ_H 2.38), H$_3$-13 (δ_H 1.43) and H$_3$-15 (δ_H 1.24), and the missing correlation of H-6 and H$_3$-15 (δ_H 1.24) defined the relative β-orientation of H-6 (► **Fig. 4** and **Fig. 11 aS**, Supporting Information). Hence, **2** was unequivocally identified and trivially named peroxyhirsutofolin A.

Positive-ion ESI-HRMS of compound **3** indicated a molecular formula of $C_{31}H_{46}O_5$ due to pseudomolecular ion at m/z 499.3424 [M + H]$^+$. The NMR data of **3** (► **Table 1**) were again very similar to those of **1**, and differences were only observed for the signals of the acyl moiety. In the ^{1}H NMR spectrum, a typical triplet for H$_3$-4′ (δ_H 0.80) and a doublet for H$_3$-5′ (δ_H 1.00) were detected and hinted the existence of a 2-methylbutyryl side chain. This was also in accordance with the pseudomolecular ion's mass pointing to an additional methylene group compared to **1**. The relative stereochemistry of **3** was determined to be identical to that of **1** and **2** by NOESY data and the hitherto unknown **3** henceforth called hirsutofolin B, being a 2-methylbutyryl analog of hirsutofolin A (**1**).

▶ Table 1 ^1H and ^{13}C NMR (600 or 150 MHz, CDCl$_3$, δ in ppm, J in Hz) data for compounds **1–4**.

| C/H	1 δ$_C$	1 δ$_H$ (H, mult, J in Hz)	2 δ$_C$	2 δ$_H$ (H, mult, J in Hz)	3 δ$_C$	3 δ$_H$ (H, mult, J in Hz)	4 δ$_C$	4 δ$_H$ (H, mult, J in Hz)
1	87.3		87.3		87.5		86.0	
2	205.2		205.1		205.3		204.1	
3	67.8		67.7		67.9		67.5	
4	208.2		208.1		208.3		204.5	
5	70.9		70.2		70.9		68.1	
6	49.4	1.83 (1H, m)	43.4	2.38 (1H, dd, 9.2, 10.6)	49.5	1.84 (1H, m)	52.0	2.09 (1H, dd, 7.6, 11.3)
7	29.4	1.90 (1H, m) 1.84 (1H, m)	28.6	1.84 (2H, m)	29.5	1.88 (2H, m)	29.3	1.87 (1H, m)
8	43.4	1.89 (1H, m)	43.2	1.42 (1H, m)	43.4	1.88 (1H, m)	42.8	1.93 (1H, t, 6.7)
9	47.4		47.2		47.6		47.3	
10	38.0	2.51 (1H, dd, 14.2, 6.0) 1.79 (1H, d, 14.2)	37.0	2.53 (1H, dd, 6.6, 14.3) 1.84 (1H, m)	38.4	2.49 (1H, dd, 5.9, 14.4) 1.79 (1H, d, 14.4)	35.8	2.52 (1H, m) 1.87 (1H, m)
11	206.2		205.3		206.0		201.3	
12	75.9		87.3		75.9		76.4	
13	26.8	1.40 (3H, s)	21.7	1.43 (3H, s)	26.6	1.39 (3H, s)	24.0	1.39 (3H, s)
14	33.0	1.34 (3H, s)	26.7	1.31 (3H, s)	33.0	1.32 (3H, s)	32.7	1.26 (3H, s)
15	22.5	1.25 (3H, s)	22.5	1.24 (3H, s)	22.7	1.26 (3H, s)	21.9	1.26 (3H, s)
16	24.8	1.25 (3H, s)	24.8	1.25 (3H, s)	24.7	1.22 (3H, s)	24.6	1.26 (3H, s)
1′	209.0		209.1		208.5		207.0	
2′	43.0	2.04 (1H, sept, 6.5)	43.0	2.03 (1H, sept, 6.1)	50.1	1.70 (1H, m)	50.8	1.63 (1H, m)
3′	20.7	1.13 (3H, d, 6.5)	20.7	1.13 (3H, d, 6.4)	26.6	1.98 (1H, ddd, 2.0, 7.3, 13.8) 1.30 (1H, ddd, 2.8, 7.1, 14.0)	26.2	1.87 (1H, m) 1.33 (1H, m)
4′	21.7	1.01 (3H, d, 6.5)	21.7	1.00 (3H, d, 6.4)	11.6	0.80 (3H, t, 7.5)	11.6	0.78 (3H, t, 7.4)
5′					17.7	1.00 (3H, d, 6.5)	16.8	1.08 (3H, d, 6.5)
1″	28.7	2.55 (1H, m)	28.6	2.56 (2H, d, 7.4)	28.9	2.53 (2H, dd, 1.9, 6.8)	28.5	2.54 (2H, m)
2″	119.0	5.21 (1H, tt, 7.3, 1.4)	119.0	5.23 (1H, t, 7.4)	119.1	5.17 (1H, t, 7.2)	118.6	5.24 (1H, t, 7.3)
3″	135.2		135.3		135.0		135.8	
4″	18.0	1.68 (3H, s)	18.0	1.68 (3H, s)	18.0	1.68 (3H, s)	18.1	1.66 (3H, s)
5″	26.0	1.72 (3H, s)	26.0	1.72 (3H, s)	26.1	1.70 (3H, s)	26.1	1.73 (3H, s)
1‴	34.1	3.19 (2H, m)	32.4	3.21 (1H, dd, 10.3, 13.8) 3.06 (1H, dd, 3.6, 14.5)	34.1	3.17 (2H, d, 8.0)	127.1	6.68 (1H, d, 16.6)
2‴	119.9	4.51 (1H, m)	120.1	4.50 (1H, m)	119.7	4.50 (1H, t, 7.2)	134.1	5.72 (1H, d, 16.6)
3‴	136.7		136.6		136.2		82.0	
4‴	18.1	1.61 (3H, s)	18.2	1.61 (3H, s)	18.1	1.61 (3H, s)	24.9	1.26 (3H, s)
5‴	25.7	1.50 (3H, s)	25.7	1.50 (3H, s)	26.0	1.51 (3H, s)	25.1	1.30 (3H, s)

Positive-ion ESI-HRMS of compound **4** indicated a molecular formula of C$_{31}$H$_{46}$O$_7$ due to pseudomolecular ion at *m/z* 553.3139 [M + Na]$^+$. The most notable signals in the ^1H NMR spectrum of **4** were a pair of vinyl doublets at δ$_H$ 6.68 (H-1‴) and 5.72 (H-2‴). Due to the large coupling constant (J$_{1‴, 2‴}$ = 16.6 Hz), a *trans*-substituted double bond could be assumed. Conspicuous was the close coincidence of the NMR data with those of **3** (▶ **Table 1**). Extensive structure elucidation revealed an analog of
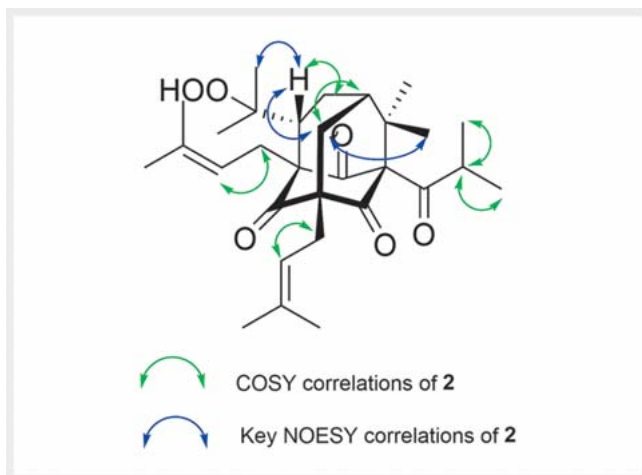
▶ **Fig. 4** Key COSY and NOESY correlations of **2**.

3 with a peroxide group at C-3‴ (δ_C 82.0) and a shifted double bond to C-1‴/C-2‴ (δ_C 127.1/134.1). This moiety was also found in 33-hydroperoxyisoplekentione C, a constituent of *C. havetiodes* var. *stenocarpa* [26]. NOE correlations of H_a – 10 (δ_H 2.52) and H_3-16 (δ_H 1.26), H_b-10 (δ_H 1.87) and H-6 (δ_H 2.09), and the lacking cross-peak between H-6 and H_3-16 (δ_H 1.26) were indicative of the β-orientation of H-6 (**Fig. 16S** and **17S**, Supporting Information) and thus proved the same stereochemistry compared to **1–3**. Based on these data, compound **4** was identified and henceforth called 3‴-hydroperoxyisohirsutofolin B.

Compound **5** was isolated as a colorless oil and displayed a positive ESI-HRMS pseudomolecular ion at *m/z* 499.3426 [M + H]⁺, consistent with a molecular formula of $C_{31}H_{46}O_5$. Most of the HMBC correlations observed for the previous substances were also found in **5** (**Fig. 21S–23 aS**, Supporting Information) and revealed the presence of the homoadamantane scaffold, a 2-methylbutyryl side chain, and 2 isopentenyl moieties at C-3 (δ_C 58.5) and C-5 (δ_C 66.3). However, in contrast to **1–4**, only 3 ketone carbons C-2 (δ_C 209.0), C-11 (δ_C 205.2) and C-1' (δ_C 209.3) were observed whereas a nonprotonated carbon replaced the fourth at δ_C 109.8 (C-4). This chemical shift indicated the replacement of the carbonyl group by a hemiketal formed by the reaction of the keto functionality at C-4 with the hydroxyl group at C-12. Remarkable was also the downfield shifted resonance of C-12 (δ_C 83.4, compared to δ_C 75.9 in **3**). These NMR data (▶ **Table 2**), together with the molecular formula, led to the conclusion that there was a fourth ring system, a tetrahydrofuran ring, comprising C-4 (δ_C 109.8), C-5 (δ_C 66.3), C-6 (δ_C 52.4), C-12 (δ_C 83.4), and an oxygen atom. The relative stereochemistry was deduced from NOESY data (**Fig. 24S** and **25S**, Supporting Information). Cross peaks between H-10b (δ_H 2.14) and H_3-13 (δ_H 1.43) and between H-10a (δ_H 2.18) and H_3-16 (δ_H 1.22) determined the relative positions of the 2 geminal methyl groups at C-9 and C-12 and the methylene hydrogens at C-10. The relative α-orientation of the hydrogen atom at C-6 was defined by NOESY cross-peaks between H_3-15 (δ_H 1.11) and H_a – 7 (δ_H 1.94), H-7b and H-6 (δ_H 2.35), and H-7b (δ_H 1.88) and H_3-13. Thus, compound **5** was assigned as a

hitherto unknown tetracyclic polyprenyl homoadamantane acylphloroglucinol derivative and trivially named hirsutuman B. A similar substance with aromatic acyl moiety, sampsonione B, was isolated from *H. sampsonii* Hance [14] and *C. obdeltifolia* Bittrich [24].

Compound **6** was isolated as a colorless oil, and its molecular formula was assigned to be $C_{30}H_{44}O_6$ by positive-ion ESI-HRMS showing a pseudomolecular ion at *m/z* 501.3214 [M + H]⁺. The ¹H and ¹³C NMR data of **6** (▶ **Table 2**) closely resembled those of **5**. A noticeable difference was observable for the acyl group, which could easily be identified as an isobutyryl moiety. Furthermore, instead of the olefinic nonprotonated carbon at δ_C 134.3 (C-3‴ in **5**) and a methylene carbon at δ_C 36.4 (C-1‴ in **5**) in the isoprene moiety at position 5, an oxygenated tertiary carbon at δ_C 71.2 (C-3‴) and an olefinic methine carbon at δ_C 125.7 (C-1‴) appeared in **6**, thereby revealing hydroxylation of C-3‴ and migration of the double bond to C-1‴/C-2‴. The large coupling constant ($J_{1'', 2''}$ = 16.3 Hz) confirmed the *trans* substitution of the double bond. The relative stereochemistry is according to the very rigid skeleton comparable with that of compound **5**. Hence, compound **6** was unequivocally identified as a hitherto undescribed tetracyclic homoadamantane acylphloroglucinol and trivially named 3‴-hydroxyisohirsutuman A. Similar substances, hyphenrones M and N, have been isolated from *H. henryi* H. Lév. & Vaniot [27].

Compound **7** was obtained as a colorless oil. The positive-ion ESI-HRMS gave a pseudomolecular ion at *m/z* 515.3364 [M + H]⁺, corresponding to the molecular formula $C_{31}H_{46}O_6$. Due to very similar 1D and 2D NMR data (▶ **Table 2**; **Fig. 33S** and **34S**, Supporting Information), the structure of **7** was shown to be an analog of **6**, with a 2-methylbutyryl acyl side chain and thus trivially named 3‴-hydroxyisohirsutuman B.

Compound **8** was isolated as a colorless oil and yielded a pseudomolecular ion peak at *m/z* 531.3310 [M + H]⁺ in positive-ion ESI-HRMS, indicative of the molecular formula $C_{31}H_{46}O_7$. In addition to NMR signals for the homoadamantyl skeleton with a 2-methylbutyryl as starter acid and an isopentenyl moiety at C-3, 2 characteristic deshielded C-atoms, C-12 (δ_C 88.4) and C-2‴ (δ_C 89.1) were observed. Geminal methyl groups H_3-13 (δ_H 1.04), H_3-14 (δ_H 1.29), and H-6 (δ_H 2.76) showed strong correlations to C-12, whereby the linkage of an isopropyl unit to the main core at C-6 could be confirmed. HMBC cross-peaks could also be detected between both geminal methyl groups H_3-4‴ (δ_H 1.24) and H_3-5‴ (δ_H 1.20) and the methylene H_a-1‴ (δ_H 3.41) and C-2‴, between H_3-4‴/H_3-5‴ and C-3‴ (δ_C 73.2), and between H_2-1‴ (δ_H 1.48 and 3.41) and numerous C-atoms (C-4 [δ_C 204.7], C-5 [δ_C 66.6], C-11 [δ_C 207.3], C-2‴ [δ_C 89.1], and C-3‴ [δ_C 73.2], **Fig. 38S** and **39S**, Supporting Information). The downfield shifted signal of C-3‴ was typical for nonprotonated C-atoms with a hydroxyl and geminal methyl groups. Based on these data, a hydroxyisopentanyl moiety located at C-5 could be assumed. The molecular formula and the deshielded resonances of C-12 and C-2‴ indicated a peroxide bridge to link these carbons. The close coincidence of the NMR data (▶ **Table 3**) to those of plukenetione C, a constituent of *C. plukenetii* Urb. [28], confirmed the proposed structure of **8**. Examination of the NOESY spectrum (**Fig. 40S** and **41S**, Supporting Information) yielded cross-peaks of H-10a (δ_H 2.48) and H_3-16 (δ_H 1.30), H_3-15 (δ_H 1.26) and H-6 (δ_H 2.76), and H-10b (δ_H 1.76) and H_3-13 (δ_H 1.04), which, together with the absence of a NOE

▶ **Table 2** ^1H and ^{13}C NMR (600 or 150 MHz, CDCl$_3$, δ in ppm, J in Hz) data for compounds **5–7**.

C/H	5		6		7	
	δ$_C$	δ$_H$ (H, mult, J in Hz)	δ$_C$	δ$_H$ (H, mult, J in Hz)	δ$_C$	δ$_H$ (H, mult, J in Hz)
1	86.0		85.0		84.9	
2	209.0		208.8		208.8	
3	58.5		58.4		58.4	
4	109.8		108.2		108.3	
5	66.3		67.4		67.5	
6	52.4	2.35 (1H, m)	52.8	2.60 (1H, dd, 1.4, 7.2)	52.9	2.59 (1H, dd, 1.1, 7.2)
7	25.7	1.94 (1H, dd, 8.5, 16.5) 1.88 (1H, dd, 7.6, 16.5)	25.4	1.97 (2H, m)	25.6	1.97 (2H, dd, 9.1, 9.1)
8	43.3	1.61 (1H, m)	43.1	1.64 (1H, m)	43.2	1.63 (1H, m)
9	46.9		46.9		47.2	
10	32.0	2.18 (1H, m) 2.14 (1H, m)	32.6	2.22 (1H, dd, 6.1, 14.7) 2.13 (1H, dd, 1.4, 15.2)	32.5	2.22 (1H, dd, 6.2, 15.2) 2.12 (1H, dd, 1.1, 14.9)
11	205.2		203.2		203.4	
12	83.4		84.0		84.1	
13	28.2	1.43 (3H, s)	27.0	1.42 (3H, s)	27.1	1.42 (3H, s)
14	33.3	1.58 (3H, s)	33.0	1.53 (3H, s)	33.1	1.52 (3H, s)
15	22.1	1.11 (3H, s)	21.8	1.12 (3H, s)	22.0	1.11 (3H, s)
16	24.7	1.22 (3H, s)	24.3	1.22 (3H, s)	24.5	1.23 (3H, s)
1′	209.3		208.4		208.2	
2′	50.1	1.83 (1H, ddd, 2.9, 6.6, 9.6)	43.2	1.96 (1H, m)	49.8	1.74 (1H, m)
3′	26.2	2.03 (1H, m) 1.33 (1H, m)	20.2	1.14 (3H, d, 6.5)	26.1	1.90 (1H, m) 1.32 (1H, m)
4′	11.6	0.85 (3H, t, 7.5)	21.0	0.94 (3H, d, 6.6)	11.6	0.83 (3H, t, 7.4)
5′	17.2	0.99 (3H, d, 6.5)			16.8	0.94 (3H, d, 6.6)
1″	27.9	2.61 (1H, dd, 6.0, 14.2) 2.34 (1H, dd, 8.3, 14.9)	28.4	2.67 (1H, dd, 6.5, 14.3) 2.37 (1H, dd, 8.6, 14.3)	28.3	2.67 (1H, dd, 6.1, 14.4) 2.37 (1H, dd, 8.9, 14.4)
2″	120.1	5.37 (1H, t, 7.7)	120.1	5.41 (1H, t, 7.6)	120.2	5.39 (1H, t, 7.5)
3″	134.9		135.1		135.0	
4″	17.8	1.64 (3H, s)	17.8	1.66 (3H, s)	17.9	1.66 (3H, s)
5″	26.0	1.72 (3H, s)	26.1	1.73 (3H, s)	26.0	1.73 (3H, s)
1‴	36.4	3.01 (1H, dd, 4.0, 15.0) 2.85 (1H, dd, 8.6, 15.0)	125.7	6.36 (1H, d, 16.3)	125.9	6.35 (1H, d, 16.3)
2‴	121.6	5.35 (1H, t, 8.3)	143.6	6.04 (1H, d, 16.3)	143.5	6.03 (1H, d, 16.3)
3‴	134.3		71.2		71.4	
4‴	17.9	1.68 (3H, s)	29.4	1.34 (3H, s)	29.5	1.34 (3H, s)
5‴	26.2	1.66 (3H, s)	29.9	1.35 (3H, s)	29.9	1.35 (3H, s)

interaction between H-6 and H$_2$-10, allowed assignment of H-6 as α-orientated. Due to a strong NOE correlation between H-6 and H-2‴, α-orientation of H-2‴ was confirmed. Hence, compound **8** was assigned as a hitherto unknown homoadamantane acylphlor-oglucinol endoperoxide and trivially named hyperihirsan B. Structurally related compounds were also found in *H. sampsonii* Hance [22, 25], *H. erectum* Thunb. [21], *H. attenuatum* Fischer ex Choisy [29], and *C. havetiodes* var. *stenocarpa* [26].

▶ **Table 3** ^{1}H and ^{13}C NMR (600 or 150 MHz, CDCl$_3$, δ in ppm, J in Hz) data for compounds **8–10**.

C/H	8		9		10	
	δ$_C$	δ$_H$ (H, mult, J in Hz)	δ$_C$	δ$_H$ (H, mult, J in Hz)	δ$_C$	δ$_H$ (H, mult, J in Hz)
1	86.3		86.0		86.0	
2	204.2		206.4		206.4	
3	68.0		55.9		55.9	
4	204.7		109.7		109.6	
5	66.6		62.7		62.7	
6	42.7	2.76 (1H, dd, 8.1, 10.8)	41.8	2.68 (1H, m)	41.8	2.67 (1H, m)
7	31.4	2.37 (1H, ddd, 4.8, 10.8, 15.4) 1.44 (1H, m)	25.8	2.04 (1H, dd, 11.0, 17.8) 1.90 (1H, dd, 7.5, 17.8)	25.8	2.05 (1H, m) 1.90 (1H, m)
8	44.2	1.99 (1H, m)	45.4	1.70 (1H, m)	45.5	1.69 (1H, m)
9	49.5		47.3		47.5	
10	40.7	2.48 (1H, dd, 6.1, 14.3) 1.76 (1H, m)	31.6	2.28 (1H, dd, 6.6, 15.0) 2.14 (1H, d, 15.0)	31.7	2.28 (1H, dd, 6.6, 15.0) 2.14 (1H, m)
11	207.3		208.6		208.5	
12	88.4		82.9		82.9	
13	17.8	1.04 (3H, s)	27.0	1.52 (3H, s)	27.0	1.52 (3H, s)
14	28.2	1.29 (3H, s)	32.1	1.43 (3H, s)	32.1	1.43 (3H, s)
15	22.6	1.26 (3H, s)	22.1	1.08 (3H, s)	24.5	1.24 (3H, s)
16	24.6	1.30 (3H, s)	24.5	1.25 (3H, s)	28.1	1.08 (3H, s)
1′	206.6		209.7		209.4	
2′	50.0	1.73 (1H, m)	41.9	2.39 (1H, sept, 6.5)	48.3	2.13 (1H, m)
3′	26.8	1.84 (1H, ddd, 2.4, 7.4, 13.4) 1.32 (1H, m)	20.2	1.12 (3H, d, 6.5)	26.2	1.94 (1H, m) 1.34 (1H, m)
4′	11.7	0.83 (3H, t, 7.4)	21.1	1.06 (3H, d, 6.5)	11.2	0.82 (3H, t, 7.5)
5′	17.2	1.01 (3H, d, 6.6)			17.2	1.06 (3H, d, 6.5)
1″	29.6	2.55 (2H, m)	27.5	2.72 (1H, dd, 4.8, 14.9) 2.37 (1H, m)	27.5	2.72 (1H, dd, 4.8, 14.9) 2.37 (1H, dd, 9.3, 14.9)
2″	119.0	5.08 (1H, t, 6.8)	119.4	5.26 (1H, t, 7.4)	119.5	5.25 (1H, m)
3″	135.1		134.8		134.7	
4″	18.1	1.68 (3H, s)	18.0	1.62 (3H, s)	18.0	1.71 (3H, s)
5″	26.0	1.70 (3H, s)	26.0	1.71 (3H, s)	26.0	1.62 (3H, s)
1‴	30.1	3.41 (1H, dd, 11.6, 15.0) 1.48 (1H, dd, 2.8, 15.0)	37.7	2.65 (1H, dd, 7.9, 13.7) 2.56 (1H dd, 7.9, 13.4)	37.7	2.63 (1H, dd, 7.7, 13.5) 2.56 (1H, dd, 8.0, 13.5)
2‴	89.1	4.76 (1H, dd, 2.8, 11.6)	84.0	4.30 (1H, t, 7.8)	84.0	4.30 (1H, t, 7.8)
3‴	73.2		70.3		70.2	
4‴	24.9	1.24 (3H, s)	24.8	1.08 (3H, s)	25.0	1.08 (3H, s)
5‴	25.9	1.20 (3H, s)	27.9	1.28 (3H, s)	27.8	1.27 (3H, s)

Compound **9**, a colorless oil, had the molecular formula C$_{30}$H$_{44}$O$_7$ as determined by positive-ion ESI-HRMS with a pseudo-molecular ion at *m/z* 517.3169 [M + H]$^+$. The NMR data for **9** (▶ **Table 3**) were very similar to that of **8** but showed signals for an isobutyryl group as an acyl side chain. The salient difference between the NMR data of both compounds was the signal of C-4 resonating at δ$_C$ 109.7 in **9** instead of δ$_C$ 204.7 in **8**. Similarly, to **5**, a hemiketal structure at C-4 was supposed. Thus, an additional tetrahydropyran moiety, comprising C-4, C-5, C-1‴, C-2‴, C-3‴, and an oxygen atom was built. Due to the inflexible, complex

caged pentacyclic scaffold, stereochemistry is very restricted. Deduced from NOE correlations comparable with those observed in **8**, H-6 (δ_H 2.68) had to be α-oriented. Because of the strong ring strain, H-2‴ and OH-4 had to be in α position, too. Thus, compound **9** was assigned as a hitherto unknown hemiketal derivative of the hyperihirsan type with isobutyryl side chain and consequently named pyranohyperihirsan A.

Compound **10** was obtained as a colorless oil. Positive-ion ESI-HRMS indicated a molecular formula of $C_{31}H_{46}O_7$ due to a pseudomolecular ion at *m/z* 531.3319 [M + H]⁺. A remarkable resemblance between the NMR data of **10** (▶ **Table 3**) and those of **9** was detected. Thus, **10** was proposed to differ from **9** only by an additional methylene group. The occurrence of a doublet and a triplet at high field (around 1 ppm) in the ¹H NMR spectrum and all relevant HMBC cross-peaks suggested that the acyl side chain was a 2-methylbutyryl moiety compared with the isobutyryl group in **9**. Analysis of the NOESY data also revealed the same relative stereochemistry as for **9,** and thus the structure of compound **10**, named pyranohyperihirsan B, was unequivocally identified.

Compound **11**, a colorless oil, has a molecular formula $C_{30}H_{44}O_5$ evidenced by positive-ion ESI-HRMS showing a pseudomolecular ion at *m/z* 485.3260 [M + H]⁺. Apart from the homoadamantane scaffold with an isobutyryl side chain and an isopentenyl group in position 3, the elucidation of the structure with NMR (▶ **Table 4**) yielded the presence of an additional cyclopentan ring. This assumption was supported by the loss of the second olefinic hydrogen in comparison to **1** and the presence of HMBC correlations between H₂-1‴ (δ_H 2.40/2.66) and the nonprotonated carbons C-4 (δ_C 205.3), C-5 (δ_C 73.3), C-11 (δ_C 203.8), C-12 (δ_C 47.0), and C-3‴ (δ_C 73.4) and the 2 methine carbons C-6 (δ_C 54.8) and C-2‴ (δ_C 59.1). Furthermore, HMBC cross-peaks between H-6 (δ_H 2.26) and C-12 as well as the geminal methyl groups C-13 (δ_C 26.9) and C-14 (δ_C 27.3) could be detected. The geminal methyl groups H₃-4‴ (δ_H 1.40) and H₃-5‴ (δ_H 1.39) correlated to each other as well as to C-2‴ and C-3‴, the latter being downfield shifted due to an attached hydroxyl group. HMBC correlation from C-3‴ to H₃-5‴ established the attachment of a 2-(2-hydroxy)propyl at C-2‴ (**Fig. 48S** and **49S**, Supporting Information). The relative stereochemistry of the chiral centers C-6 and C-2‴ were established by NOE correlations. Cross peaks between H-10a (δ_H 2.38) and H₃-16 (δ_H 1.25), H-7a (δ_H 1.96), and H₃-15 (δ_H 1.26) and between H-6 (δ_H 2.26) and H-10b (δ_H 2.09) disclosed the β orientation of H-6. The 2-(2-hydroxyl)propyl unit at C-2‴ was likewise determined to be β orientated due to key NOESY correlations of H₃-14 (δ_H 1.21) with H-6, and of H₃-13 (δ_H 1.10) with H-7a (δ_H 1.96) and H-2‴ (δ_H 2.20) (**Fig. 50S** and **51S**, Supporting Information). Hence, compound **11** was identified as a hitherto unknown homoadamantane acylphloroglucinol derivative with an additional cyclopentane ring and trivially named hirsutal A. Structurally related substances could be found in the literature [27, 30, 31].

Compound **12** was isolated as a colorless oil and yielded a pseudomolecular ion peak at *m/z* 499.3416 [M + H]⁺ in positive-ion ESI-HRMS, indicative of the molecular formula $C_{31}H_{46}O_5$. The NMR spectra for **12** were very similar to that of **11** but showed signals for a 2-methylbutyryl group as an acyl side chain (▶ **Table 4**).

Consequently, **12** could be identified as the 2-methylbutyryl analog of **11** and henceforth named hirsutal B.

Compounds **13** and **14** were isolated as a mixture of 2 diastereomers, and their formula was assigned to be $C_{31}H_{46}O_5$ by positive-ion ESI-HRMS showing a pseudomolecular ion at *m/z* 499.3420 [M + H]⁺. Examination of the NMR data (▶ **Table 4**) yielded the same carbon skeleton as for **12**. Conspicuous was a more or less distinct chemical shift of some carbon atoms, especially C-7, C-10, C-13, and C-14. Detailed observation of the relative stereochemistry at C-6 and C-2‴ revealed some differences. For **13**, the NOESY spectrum showed correlations of H-10a (δ_H 2.45) and H₃-16 (δ_H 1.30), H₃-15 (δ_H 1.28), and H-7a (δ_H 2.22), as well as H-6 (δH 2.03), and thereby, indicated the α position of H-6. The relative configuration of H-2‴ was ascertained by NOE cross-peaks between H₃-14 (δ_H 1.21) and both H-7a and H-6 and between H₃-13 (δ_H 0.89) and H-7b (δ_H 1.57), H-10b (δ_H 1.77), and H-2‴ (δ_H 2.47) as β-oriented. This configuration is known from sampsonione C [29, 30], attenuatumione A [32], and plukenetione B [28, 31]. Comparable to **11** and **12**, the NOESY spectrum showed for **14** correlations of H-10a (δ_H 2.37) and H₃-16 (δ_H 1.26), H₃-15 (δ_H 1.26), and H-7a (δ_H 1.91) and also of H-6 (δ_H 1.82) and H-10b (δ_H 2.10), which established the relative β orientation of H-6. Also, a cross-peak from H₃-13 (δ_H 1.05) to H$_a$-7 was present, but this time H-2‴ (δ_H 1.81), H-6, and H$_b$-7 (δ_H 1.63) were correlating to H₃-14 (δ_H 1.11), thereby all revealing β orientation (**Fig. 56S–57 aS**, Supporting Information). The hitherto undescribed derivatives **13** and **14** were trivially named hirsutals C and D. Related compounds were isolated from *H. cohaerens* N. Robson [31], *H. henryi* H. Lév. & Vaniot [27], and *H. attenuatum* Fischer ex Choisy [32].

Compound **15** was isolated as a colorless oil and displayed a positive ESI-HRMS ion at *m/z* 483.3110 [M + H]⁺, consistent with a molecular formula of $C_{30}H_{42}O_5$. Besides the adamantane scaffold and an isobutyryl acyl side chain, ¹H NMR spectrum of **15** showed 2 olefinic protons H-2″ (δ_H 5.18) and H-2‴ (δ_H 5.03) belonging to 2 isopentenyl moieties (▶ **Table 5**). HMBC analysis (**Fig. 60S, 62S**, and **63S**, Supporting Information) yielded the reported cross-peaks for C-3 (δ_C 68.5) and C-5 (δ_C 70.2). The geminal methyl groups H₃-13 (δ_H 1.19) and H₃-14 (δ_H 1.31) showed HMBC correlations to each other (δ_C 19.4 and 24.3), the methine carbon C-11 (δ_C 60.7), and the non-protonated carbon C-12 (δ_C 61.2). The molecular formula indicated an additional oxygen in the structure of **15,** and together with the deshielded positions of C-11 and C-12, the presence of an 11,12-oxiran moiety can be assumed. Out of the 6 asymmetric carbons (C-1, C-3, C-5, C-6, C-7, and C-11), the configuration of the bridgehead carbons C-1, C-3, C-5, and C-7 was obviously determined by the rigid adamantane backbone. Analysis of NOESY data (**Fig. 64S** and **65S**, Supporting Information) showed α-orientation of H-6. The proton correlated with H₃-15 (δ_H 1.32) but not with H₂-9 (δ_H 2.51). Due to free rotation around the C-6/C-11 bond, the determination of the stereochemistry at C-11 was awkward. Ye et al. [33] showed that adamantane-type acylphloroglucinols with an 11,12-epoxide moiety could be divided into 2 groups. The first contains compounds with β-orientation for H-11 showing a chemical shift of ~ 58 ppm for C-12, while the second group involves compounds with α-oriented H-11 exhibiting a chemical shift ~ 62 ppm for C-

▶ **Table 4** ¹H and ¹³C NMR (600 or 150 MHz, CDCl₃, δ in ppm, J in Hz) data for compounds **11–14**.

C/H	11		12		13		14	
	δ_C	δ_H (H, mult, J in Hz)	δ_C	δ_H (H, mult, J in Hz)	δ_C	δ_H (H, mult, J in Hz)	δ_C	δ_H (H, mult, J in Hz)
1	85.8		85.6		86.0		85.2	
2	204.4		204.4		204.7		204.7	
3	67.3		67.3		68.6		67.1	
4	205.3		205.4		206.0		203.2	
5	73.3		73.3		73.3		70.8	
6	54.8	2.26 (1H, dd, 7.4, 12.6)	54.8	2.25 (1H, dd, 7.4, 12.5)	57.6	2.03 (1H, m)	56.6	1.82 (1H, m)
7	24.6	1.96 (1H, m) 1.70 (1H, m)	24.6	1.96 (1H, m) 1.69 (1H, m)	28.7	2.22 (1H, m) 1.57 (1H, m)	22.5	1.91 (1H, m) 1.63 (1H, m)
8	42.1	1.98 (1H, m)	42.2	1.97 (1H, m)	43.7	2.02 (1H, m)	42.0	1.99 (1H, m)
9	47.0		47.1		50.0		47.2	
10	35.1	2.38 (1H, m) 2.09 (1H, d, 14.8)	35.1	2.37 (1H, m) 2.08 (1H, d, 14.8)	42.0	2.45 (1H, m) 1.77 (1H, m)	35.0	2.37 (1H, dd, 6.6, 14.8) 2.10 (1H, m)
11	203.8		203.7		203.4		202.6	
12	47.0		46.9		44.9		46.4	
13	26.9	1.10 (3H, s)	26.9	1.10 (3H, s)	27.3	0.89 (3H, s)	17.4	1.05 (3H, s)
14	27.3	1.21 (3H, s)	27.4	1.21 (3H, s)	28.4	1.21 (3H, s)	29.6	1.11 (3H, s)
15	22.4	1.26 (3H, s)	22.5	1.27 (3H, s)	22.6	1.28 (3H, s)	22.4	1.26 (3H, s)
16	24.9	1.25 (3H, s)	24.9	1.25 (3H, s)	25.2	1.30 (3H, s)	25.1	1.26 (3H, s)
1′	207.5		207.1		207.6		207.1	
2′	43.0	1.91 (1H, sept, 6.5)	49.5	1.66 (1H, m)	49.8	1.74 (1H, m)	49.5	1.64 (1H, m)
3′	20.3	1.05 (3H, d, 6.6)	26.5	1.76 (1H, m) 1.28 (1H, m)	26.8	1.96 (1H, m) 1.31 (1H, m)	26.5	1.76 (1H, m) 1.27 (1H, m)
4′	20.8	1.01 (3H, d, 6.6)	11.6	0.81 (3H, t, 7.4)	11.7	0.84 (3H, t, 7.5)	11.5	0.80 (3H, t, 7.5)
5′			16.9	0.97 (3H, d, 6.6)	16.8	0.96 (3H, d, 6.4)	16.9	1.04 (3H, d, 6.4)
1″	29.0	2.53 (1H, m)	29.1	2.53 (1H, m)	29.6	2.51 (2H, m)	29.0	2.55 (2H, m)
2″	118.7	5.20 (1H, t, 7.4)	118.7	5.19 (1H, t, 7.3)	119.3	5.07 (1H, t, 6.9)	118.8	5.24 (1H, t, 7.4)
3″	135.4		135.4		134.6		135.3	
4″	18.0	1.65 (3H, s)	18.0	1.65 (3H, s)	18.1	1.68 (3H, s)	18.0	1.66 (3H, s)
5″	26.1	1.72 (3H, s)	26.1	1.73 (3H, s)	26.0	1.69 (3H, s)	26.1	1.74 (3H, s)
1‴	30.5	2.66 (1H, dd, 6.7, 14.3) 2.40 (1H, dd, 8.6, 14.3)	30.5	2.66 (1H, dd, 6.9, 14.4) 2.38 (1H, dd, 2.9, 14.4)	32.8	2.50 (1H, m) 2.11 (1H, m)	29.9	2.65 (1H, m) 2.43 (1H, m)
2‴	59.1	2.20 (1H, t, 7.5)	59.1	2.21 (1H, t, 7.6)	57.4	2.47 (1H, m)	59.2	1.81 (1H, m)
3‴	73.4		73.4		73.4		72.8	
4‴	30.5	1.40 (3H, s)	30.5	1.40 (3H, s)	30.4	1.39 (3H, s)	30.6	1.40 (3H, s)
5‴	31.8	1.39 (3H, s)	31.8	1.39 (3H, s)	30.1	1.33 (3H, s)	31.1	1.35 (3H, s)

12. In **15**, the C-12 resonance was at 61.2 ppm, so H-11 could be determined as α-oriented. According to [33], **15** is a known constituent from *H. hookerianum* Wight & Arn., named hookerione C. Similar compounds are also known for *H. sampsonii* Hance [13, 34].

Compound **16** was obtained as a colorless oil. The positive-ion ESI-HRMS gave a pseudomolecular ion at *m/z* 497.3263 [M + H]⁺,

corresponding to the molecular formula $C_{31}H_{44}O_5$. The ¹H NMR spectrum of **16** (▶ **Table 5**; **Fig. 66S**, Supporting information) indicated, with a triplet at 0.85 ppm and a doublet at 1.12 ppm, the presence of a 2-methylbutyryl acyl side chain instead of the isobutyryl group in **15**. NOESY correlations and a chemical shift of 61.2 ppm for C-12 resulted in the same stereochemistry for both polycyclic polyprenylated acylphloroglucinols **15** and **16**.

Table 5 ^{1}H and ^{13}C NMR (600 or 150 MHz, CDCl$_3$, δ in ppm, J in Hz) data for compounds 15–17.

C/H	15		16		17	
	δ$_C$	δ$_H$ (H, mult, J in Hz)	δ$_C$	δ$_H$ (H, mult, J in Hz)	δ$_C$	δ$_H$ (H, mult, J in Hz)
1	87.1		86.8		86.4	
2	201.5		201.4		201.7	
3	68.5		68.5		68.2	
4	202.0		202.1		202.0	
5	70.2		70.2		72.0	
6	49.0	2.70 (1H, dd, 2.3, 8.4)	48.9	2.71 (1H, d, 8.4)	54.6	2.48 (1H, dt, 2.6, 8.3)
7	44.0	1.80 (1H, q, 2.7)	44.0	1.80 (1H, q, 2.6)	45.7	1.62 (1H, q, 2.6)
8	54.1		54.1		53.9	
9	39.7	2.51 (2H, m)	39.8	2.51 (2H, m)	40.3	2.54 (1H, dt, 2.6, 14.0) 2.22 (1H, dd, 2.6, 14.0)
10	200.9		200.9		199.9	
11	60.7	2.54 (1H, d, 8.4)	60.7	2.54 (1H, d, 8.4)	61.6	2.61 (1H, d, 8.3)
12	61.2		61.2		56.8	
13	19.4	1.19 (3H, s)	19.4	1.19 (3H, s)	19.1	1.27 (3H, s)
14	24.3	1.31 (3H, s)	24.3	1.31 (3H, s)	24.6	1.31 (3H, s)
15	22.8	1.32 (3H, s)	22.9	1.32 (3H, s)	22.7	1.29 (3H, s)
16	23.4	1.34 (3H, s)	23.4	1.34 (3H, s)	23.1	1.33 (3H, s)
1′	209.2		208.6		208.3	
2′	42.3	2.19 (1H, sept, 6.6)	48.8	1.89 (1H, m)	48.7	1.96 (1H, ddd, 2.7, 6.6, 9.4)
3′	20.6	1.14 (3H, d, 6.3)	26.8	1.88 (1H, m) 1.30 (1H, m)	26.8	1.79 (1H, ddd, 2.3, 7.5, 13.4) 1.28 (1H, m)
4′	20.6	1.15 (3H, d, 6.4)	11.7	0.85 (3H, t, 7.4)	11.8	0.85 (3H, t, 7.4)
5′			16.6	1.12 (3H, d, 6.5)	16.4	1.10 (3H, d, 6.6)
1″	27.5	2.52 (2H, m)	27.5	2.51 (2H, m)	27.3	2.52 (2H, m)
2″	118.1	5.18 (1H, t, 6.8)	118.1	5.18 (1H, t, 7.2)	118.3	5.18 (1H, t, 7.3)
3″	135.4		135.3		135.3	
4″	18.0	1.67 (3H, s)	18.0	1.67 (3H, s)	18.0	1.67 (3H, s)
5″	26.0	1.71 (3H, s)	26.0	1.71 (3H, s)	26.0	1.71 (3H, s)
1‴	25.9	2.47 (2H, d, 6.6)	25.9	2.48 (2H, d, 5.9)	26.9	2.74 (1H, dd, 6.5, 15.5) 2.43 (1H, dd, 6.5, 15.5)
2‴	118.3	5.03 (1H, t, 6.4)	118.3	5.03 (1H, t, 6.3)	118.6	4.92 (1H, t, 6.4)
3‴	134.6		134.5		134.2	
4‴	18.1	1.70 (3H, s)	18.1	1.71 (3H, s)	18.2	1.74 (3H, s)
5‴	26.0	1.70 (3H, s)	26.0	1.70 (3H, s)	26.0	1.66 (3H, s)

Hence, compound 16 was identified as a hitherto unknown 2-methylbutyryl analog of hookerione C and trivially named hirsuton A.

Compound 17 was obtained as a colorless oil. Positive-ion ESI-HRMS indicated a molecular formula of C$_{31}$H$_{44}$O$_5$ due to pseudo-molecular ion at m/z 497.3263 [M + H]$^+$. Structure elucidation of 17 with NMR (▸ Table 5) gave the same planar structure as in 16.

However, there were some remarkable differences in the chemical shifts of C-6 (δ$_C$ 54.6 instead of 48.9 for 16) and C-12 (δ$_C$ 56.8 instead of 61.2 for 16) caused by the relative configuration at C-11. In this case, a β-orientation of H-11 could be determined. Thus, 17 is the C-11 epimer of 16 and henceforth called hirsuton B.

Compound 18, a colorless oil, has the molecular formula C$_{30}$H$_{44}$O$_6$ as determined by positive-ion ESI-HRMS with a quasi-

molecular ion at m/z 523.3036 $[M + Na]^+$. In addition to the adamantane scaffold with an isobutyryl acyl side chain and an isopentenyl moiety at position 3, a 5-membered carbon ring, containing C-5, C-6, C-11, C-1‴, and C-2‴, were detected by the proton spin system H$_2$-9 (δ_H 2.32/2.51)/H-7 (δ_H 1.88)/H-6 (δ_H 3.08)/H-11 (δ_H 1.99)/H-2‴ (δ_H 2.61)/H$_2$-1‴ (δ_H 1.81/2.63) in the ^{1}H-^{1}H COSY spectrum (**Fig. 75S** and **76S**, Supporting Information). This was also supported by HMBC correlations (**Fig. 74S**, Supporting Information) between H$_2$-1‴ and C-4 (δ_C 201.1), C-5 (δ_C 73.6), C-6 (δ_C 57.0), C-10 (δ_C 198.5), C-11 (δ_C 55.4), C-2‴ (δ_C 47.6), and C-3‴ (δ_C 75.3), between H-2‴ and C-5, C-6, C-11, C-1‴ (δ_C 22.8), C-3‴, C-4‴ (δ_C 25.7), and C-5‴ (δ_C 33.5), between H-11 and C-5, C-6, C-7 (δ_C 44.7), C-12 (δ_C 70.8), C-13 (δ_C 26.9), C-14 (δ_C 32.8), C-2‴, and C-3‴, and between H-6 and C-4, C-5, C-6, C-7, C-9 (δ_C 37.9), C-10, C-11, and C-2‴. Besides, cross-peaks from the geminal methyl groups H$_3$-13 (δ_H 1.35) and H$_3$-14 (δ_H 1.28) to C-11 and C-12 and from H$_3$-4‴ (δ_H 1.36) and H$_3$-5‴ (δ_H 1.36) to C-2‴ and C-3‴ together with the characteristic chemical shifts of C-12 and C-3‴ revealed that 2 2-hydroxyisopropyl units were located at C-11 and C-2‴ (NMR data in ▶ **Table 6**). The highly rigid and caged tricyclo-[3.3.1.1]-decane core determined the configuration of 4 of the 7 chiral centers C-1, C-3, C-5, and C-7. The relative stereochemistry at C-6 was deduced from the NOESY cross-peaks between H-6 and H$_3$-16 (δ_H 1.37) as well as between H-1b‴ (δ_H 1.81), H$_3$-15 (δ_H 1.38), and H-9a (δ_H 2.51) and the missing correlation between H-6 and H-9a. The NOESY correlation of H-11 to H-9b (δ_H 2.32) and H-1b‴ (δ_H 1.81) indicated β-orientation for this proton. Based on a missing cross peak from H-2‴ to H-6, H-2‴ had to be on the same side as H-11 (**Fig. 77S** and **78S**, Supporting Information). Thus, compound **18** was assigned as a hitherto unknown tetracyclic adamantan type acylphloroglucinol with isobutyryl side chain and named hyperihirsolin A. An analogous acylphloroglucinol is hyperisampsin A from *H. sampsonii* Hance [34].

Compound **19** was isolated as a colorless oil, and its molecular formula was assigned to be $C_{31}H_{46}O_6$ by positive-ion ESI-HRMS showing a pseudomolecular ion at m/z 537.3188 $[M + Na]^+$. Comprehensive NMR analyses (▶ **Table 6**) revealed compound **19** shared the same scaffold and relative configuration as **18**. The structural novelty of **19**, named hyperihirsolin B, involved the presence of a 2-methylbutyryl moiety instead of an isobutyryl moiety.

Acylphloroglucinols with adamantane and homoadamantane scaffolds are reported for the first time for *H. hirsutum* L. and section 18, *Taeniocarpium* Jaub. & Spach. Interestingly, related metabolites were hitherto mainly detected in species of the phylogenetically-related section 3 *Ascyreia* Choisy (*H. cohaerens* N. Robson, *H. henryi* H. Lév. & Vaniot, *H. pseudohenryi* N. Robson, *H. subsessile* N. Robson, *H. hookerianum* Wight & Arnott, *H. wilsonii* Robson). Further single reports on adamantane- or homoadamantane-based acylphloroglucinols have been published for section 9 *Hypericum* (*H. attenuatum* Fischer ex Choisy, *H. erectum* Thunb.) and section 9c *Sampsonia* (*H. sampsonii* Hance). Furthermore, the adamantane derivative hyperandrone A is a representative isolated from *H. androsaemum* L. (section 5 *Androsaemum* [Duhamel] Godron) [35], and according to [36], sinaicinone was discovered in *H. sinaicum* Hochst. ex Boiss. (section 27 *Adenosepalum* Spach). Adamantane backbone derived from a bicyclic acylphloroglucinol

of B1 type is found in hyperibone K of *H. scabrum* L. (section 17 *Hirtella* Stef.) [37], *H. sampsonii* Hance [38], and 18-hydroxyhyperibone K of *H. hypericoides* (L.) Cr. (section 20 *Myriandra* [Spach] R. Keller) [39]. It is of interest that most of these complex caged metabolites are synthesized by species related to sections 3 and 18 but occasionally occur in several other sections. In contrast to most other *Hypericum* species, in *H. hirsutum*, only acyl phloroglucinol with aliphatic isobutyryl or 2-methyl-butyryl side chain but no C-1 benzoylated derivatives could be found. This is noteworthy, as, among the adamantine- and homoadamantane-based acyl phloroglucinols, the benzoyl derivatives are dominating, with aliphatic derivatives being the much smaller group of metabolites.

The isolated homoadamantane derivatives **1–5**, **7**, and **10–12**, as well as the adamantane type acylphloroglucinols **15**, **16**, **18**, and **19**, and hyperforin (as positive control) were tested for their effect on the proliferation of the endothelial cell line HMEC-1. Hyperforin remarkably inhibited the proliferation of endothelial cells with an IC_{50} value of 0.8 µM. This result is comparable with literature data [40], showing a strong influence on viability in bovine aorta endothelial cells. The isolated adamantane and homoadamantane acylphloroglucinols only moderately reduced proliferation with IC_{50} values between ~ 3–22 µM (▶ **Table 7**). Both compounds showing a hydroperoxide group (**2** and **4**) were most active. An influence of the acyl group (isobutyryl versus 2-methyl-butyryl) on the antiproliferative activity was not observable. Interestingly, concentrations of adamantane and homoadamantane derivatives showing remarkable inhibition of proliferation showed no effects on the viability of the HMEC-1 in an MTT-based setup (**Fig. 88S**, Supplementary Information).

In an *in vitro* assay with human microvascular endothelial cells (HMEC-1), compounds **1–5**, **7**, and **10–12**, and hyperforin were tested for their ability to reduce the TNF-α-induced ICAM-1 expression. Compounds **12** and especially **3** reduced the ICAM-1 expression concentration-dependently (▶ **Fig. 5**). At the highest concentration (50 µM), **2** and **4**, the substances with a peroxide group, showed cytotoxic effects (**Fig. 88S**, Supplementary Information), whereas lower concentrations (25, 12.5, and 6.25 µM) showed slight or insignificant effects on the ICAM-1 expression (**Fig. 90S**, Supplementary Information). Substances **5** and **7** with an additional tetrahydrofuran subunit had only an effect at the highest concentration tested. Due to its distinct cytotoxicity on endothelial cells, hyperforin was tested in 10-fold lower concentrations (< 5 µM), showing activity at 5 µM but not at lower concentrations (**Fig. 90S**, Supplementary Information). Compounds **10**, **11** (**Fig. 90S**, Supplementary Information), and **12** showed a clear reduction of the ICAM-1 expression (62.3%) at 50 µM and slight effects at lower concentrations (▶ **Fig. 5**). The inhibitory activity regarding the nitric oxide production in LPS-activated macrophages was investigated for the most active substances in the ICAM-1 assay, **3** and **12**. The macrophages responded very sensitively as a concentration of 10 µM had cytotoxic effects for both compounds (cell viability compared to control: 47.2% for **3**, 71.9% for **12**, ▶ **Fig. 6**). Lower concentrations showed reduced cytotoxicity and no more influence on NO production. It is likely that the effect on the macrophages is thus toxicity dependent and not related to a specific NO-reducing activity.

► Table 6 ^1H and ^{13}C NMR (600 or 150 MHz, CDCl$_3$, δ in ppm, J in Hz) data for compounds **18** and **19**.

C/H		18		19
	δ$_C$	δ$_H$ (H, mult, J in Hz)	δ$_C$	δ$_H$ (H, mult, J in Hz)
1	87.6		87.6	
2	201.6		201.6	
3	67.6		67.6	
4	201.1		201.1	
5	73.6		73.6	
6	57.0	3.08 (1H, dt, 1.9, 13.2)	57.0	3.08 (1H, dt, 2.3, 13.3)
7	44.7	1.88 (1H, m)	44.7	1.87 (1H, m)
8	56.4		56.4	
9	37.9	2.51 (1H, dt, 2.7, 13.7) 2.32 (1H, m)	38.0	2.50 (1H, dt, 2.7, 13.9) 2.31 (1H, m)
10	198.5		198.5	
11	55.4	1.99 (1H, dd, 7.4, 13.7)	55.4	1.98 (1H, m)
12	70.8		70.7	
13	26.9	1.35 (3H, s)	26.8	1.35 (3H, s)
14	32.8	1.28 (3H, s)	32.8	1.28 (3H, s)
15	23.6	1.38 (3H, s)	23.6	1.37 (3H, s)
16	23.7	1.37 (3H, s)	23.7	1.38 (3H, s)
1′	209.5		209.0	
2′	42.4	2.20 (1H, sept, 6.0)	49.1	1.92 (1H, ddd, 2.7, 6.6, 9.5)
3′	20.7	1.15 (3H, d, 6.5)	26.8	1.98 (1H, m) 1.32 (1H, m)
4′	20.7	1.17 (3H, d, 6.5)	11.6	0.85 (3H, t, 7.4)
5′			16.8	1.14 (3H, d, 6.5)
1″	27.6	2.47 (2H, d, 7.3)	27.7	2.47 (2H, d, 7.3)
2″	118.1	5.16 (1H, t, 7.1)	118.2	5.15 (1H, t, 7.2)
3″	135.4		135.4	
4″	18.0	1.66 (3H, s)	18.0	1.66 (3H, s)
5″	26.0	1.71 (3H, s)	26.0	1.71 (3H, s)
1‴	22.8	2.63 (1H, dd, 10.0, 13.9) 1.81 (1H, dd, 3.5, 13.9)	22.8	2.65 (1H, dd, 10.0, 14.0) 1.81 (1H, dd, 3.9, 13.8)
2‴	47.6	2.61 (1H, m)	47.6	2.60 (1H, m)
3‴	75.3		75.3	
4‴	25.7	1.36 (3H, s)	25.7	1.36 (3H, s)
5‴	33.5	1.36 (3H, s)	33.4	1.36 (3H, s)

► Table 7 Antiproliferative activity of isolated compounds from *H. hirsutum* L. in HMEC-1 cells (IC$_{50}$ [μM], 95 % Confidence interval [μM], calculated with GraphPad Prism 5 software).

Compound	IC$_{50}$	95 % Confidence interval
1	8.2	4.1–17.4
2	2.7	0.8–7.0
3	12.4	9.1–16.4
4	4.0	0.2–6.1
5	20.1	15.9–27.8
7	12.9	4.9–26.8
10	9.5	4.4–20.7
11	8.2	3.5–18.6
12	9.2	3.9–21.4
15	15.1	12.3–19.5
16	15.5	6.9–24.4
18	21.4	13.3–31.8
19	16.2	11.4–22.9
Hyperforin	0.8	0.4–1.8

Material and Methods

General experimental procedures

For chromatography, all solvents were of analytical or HPLC grade. Water for HPLC analysis was generated with an Astacus LS (MembraPure GmbH). Diaion HP-20 (159.5 g, particle size: 250–850 μm, SUPELCO) was used for degreasing the PE extract. For crude separation, flash chromatography on a spot liquid chromatography flash device (Armen Instrument) with prepacked normal-phase column (SVP D40, Si60, 15–40 μm, 90 g, Götec-Labortechnik GmbH) was used. Centrifugal partition chromatography (CPC) was performed on a Spot CPC device with a 250 mL rotor (rotation: 800 rpm, Armen Instrument) and a 510 HPLC pump (Waters GmbH). Further separations were carried out on RP-18 material (Releveris C18-WP, 20 μm, 4 g) using a spot liquid chromatography flash device (Armen Instrument).

Isolation of the compounds was achieved on 2 semi-preparative HPLC systems. System A: binary Varian ProStar preparative HPLC (Varian Deutschland GmbH, Darmstadt, Germany) detection at 195 and 205 nm via diode array detector, manual injection. System B: binary Agilent Infinity 1260 HPLC (Agilent Technologies Sales & Services GmbH & Co. KG), 1260 Agilent fraction collector, detection at 195 and 205 nm via a 1260 Agilent diode array detector, manual injection. Separations were performed on an Eclipse XDB-C18 column (9.4 × 250 mm, 5 μm, Agilent). All collected HPLC fractions were controlled by ^1H NMR and TLC on silica gel 60 F254 (Merck) with *n*-hexane/EtOAc/formic acid 65 : 33 : 2, v/v/v as mobile phase; detection by spraying with anisaldehyde/H$_2$SO$_4$. A CAMAG TLC visualizer was used for documentation (CAMAG AG).
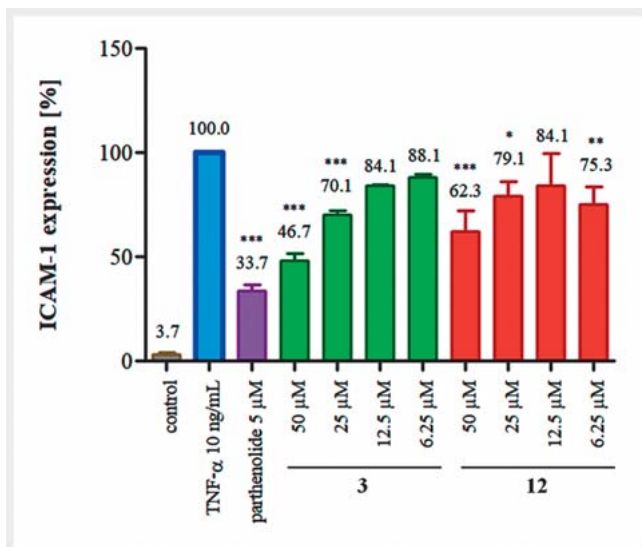
► **Fig. 5** Inhibition of TNF-α induced ICAM-1 expression in HMEC-1 cells. Control as the basal level of ICAM-1 expression, TNF-α (10 ng/mL) as the maximum level of ICAM-1 expression, and parthenolide 5 µM as the positive control. Substances **3** and **12** at different concentrations as test compounds. n = 3 in duplicates; mean ± SD; *** $p < 0.001$ vs. TNF-α, ** $p < 0.01$ vs. TNF-α, * $p < 0.05$ vs. TNF-α. Data were subjected to1-way ANOVA followed by Dunnett's post-test using GraphPad Prism 5 software.

^{1}H, ^{13}C, and 2D NMR spectra of the isolated compounds were recorded at 298 K on an AVANCE III 600 NMR (Bruker Corporation) with an operating frequency of 600.25 MHz for ^{1}H and 150.95 MHz for ^{13}C. All samples were measured in CDCl$_3$ (99.8 atom% D, Sigma-Aldrich Chemie GmbH). Chemical shifts are given in ppm (δ) and J values in Hz. Solvent signals were used as an internal reference. Structures were elucidated based on 1D and 2D (HSQC, HMBC, COSY, and NOESY) experiments. High-resolution ESI-HRMS was recorded on a Q-TOF 6540 UHD instrument (Agilent) in positive ion mode. Specific optical rotations were recorded using a UniPol L1000 polarimeter (Schmidt + Haensch GmbH & Co). A J-715 spectropolarimeter (JASCO Deutschland GmbH) was used with a 0.1 cm quartz cuvette (type: 100-QSQ, Hellma GmbH & Co. KG) to record CD-spectra at 22 °C. Each measurement was repeated 10 times, and measured intervals were from 190–400 nm with a scanning rate of 100 nm/min in 0.5 nm steps. Savitzky-Golay algorithm was used for spectra smoothing (convolution with: 15).

Plant material

The flowering aerial parts of *H. hirsutum* were collected in July 2013 at GPS coordinates 49°43′ 52.352″ N 10°3′ 23.050″ E along a forest path of the local community Biebelried. The plant was identified by Dr. Sebastian Schmidt and Prof. Dr. Jörg Heilmann (University of Regensburg). A voucher specimen is deposited at the University of Regensburg, Pharmaceutical Biology under the number JZ2013-PB.

Extraction and isolation

Through percolation with PE (8 L), dichloromethane (6 L), EtOAc (6 L), and MeOH 80% (12 L; v/v), 569 g of air-dried and powdered plant material were successively extracted. Subsequently, 15.9 g PE extract were defatted by using Diaion HP-20 column chromatography with MeOH 90% (v/v) (3.2 L, PE.1), MeOH 100% (16.0 L, PE.2), dichloromethane (3.4 L, PE.3), and PE (1 L, PE.4).

Using silica gel flash chromatography (solvent A: hexane, solvent B: EtOAc, flow rate: 30 mL/min, collection: 20 mL/vial, gradient: 0–60 min 0% → 100% B, 60–90 min 100% B), 2.1 g of PE.1 were further separated to give 5 subfractions (PE.1.1–PE.1.5). For ^{1}H NMR guided fractionation, 10 mg of every subfraction was dissolved in CDCl$_3$ and analyzed at 298 K on an AVANCE 300 NMR (Bruker Corporation) with an operating frequency of 300.13 MHz.

PE.1.3 (553.0 mg, 340–700 mL) was fractionated by CPC (rotation: 800 rpm, flow rate: 5 mL/min, collection: 5 mL/vial, upper phase: saturated n-hexane [2], lower phase: saturated MeOH/H$_2$O [1.75:0.25], ascending mode: 0–1115 mL, descending mode: 1115–1345 mL) to give 9 subfractions (PE.1.3.1–1.3.9). PE.1.3.3 (45.3 mg, 150–245 mL) was subjected to semi-preparative HPLC (system: B, flow rate: 3 mL/min, solvent A: H$_2$O, solvent B: MeCN, gradient: 0–5 min 85% B, 5–7 min 85% → 90% B, 7–25 min 90% B, 25–27 min 90% → 100% B, 27–30 min 100% B, 30–32 min 100% → 85% B, 32–35 min 85% B) to yield **11** (1.4 mg, t_R: 15.7 min), **10** (2.0 mg, t_R: 16.7 min), **12** (2.0 mg, t_R: 18.3 min), and **5** (5.4 mg, t_R: 20.9 min). Subfraction PE.1.3.4 (89.2 mg, 245–370 mL) was separated by semipreparative HPLC (system: B, flow rate: 3 mL/min, solvent A: H$_2$O, solvent B: MeCN, gradient: 0–5 min 80% B, 5–7 min 80% → 85% B, 7–12 min 85% B, 12–14 min 85% → 95% B, 14–22 min 95% B, 22–24 min 95% → 100% B, 24–27 min 100% B, 27–29 min 100% → 80% B, 29–32 min 80% B) to yield compounds **9** (2.3 mg, t_R: 17.9 min), **1** (5.2 mg, t_R: 18.6 min), a mixture of **13** and **14** (2.8 mg, t_R: 19.2 min), and **3** (34.6 mg, t_R: 20.3 min). PE.1.3.6 (22.9 mg, 520–600 mL) was applied to semi-preparative HPLC (system: B, flow rate: 3 mL/min, solvent A: H$_2$O, solvent B: MeCN, gradient: 0–5 min 80% B, 5–7 min 80% → 85% B, 7–25 min 85% B, 25–27 min 85% → 100% B, 27–32 min 100% B, 32–34 min 100% → 80% B, 34–38 min 80% B) to isolate **8** (1.4 mg, t_R: 15.9 min) and **2** (6.3 mg, t_R: 19.9 min).

PE.1.4 (533 mg, 700–1140 mL) was also further fractionated by CPC (flow rate: 5 mL/min, collection: 5 mL/vial, upper phase: saturated n-hexane/EtOAc [4:3], lower phase: saturated MeOH/H$_2$O [4:1, ascending mode: 0–1285 mL, descending mode: 1285–1780 mL) resulted in 9 subfractions (PE.1.4.1–PE.1.4.9). PE.1.4.3 (74.0 mg, 190–325 mL) was again subjected to semipreparative HPLC (system: B, flow rate: 3 mL/min, solvent A: H$_2$O, solvent B: MeCN, gradient: 0–5 min 75% B, 5–7 min 75% → 80% B, 7–20 min 80% B, 20–22 min 80% → 100% B, 22–25 min 100% B, 25–27 min 100% → 75% B, 27–30 min 75% B) to yield **18** (5.0 mg, t_R: 13.0 min), **19** (7.2 mg, t_R: 115.9 min), **7** (4.5 mg, t_R: 17.8 min), and **4** (4.1 mg, t_R: 18.6 min).

Using silica gel flash chromatography (solvent A: EtOAc, solvent B: hexane, flow rate: 30 mL/min, gradient: 0–60 min 0% → 100% A), 5.9 g of PE.2 were separated to give 6 subfractions (PE.2.1–2.6).
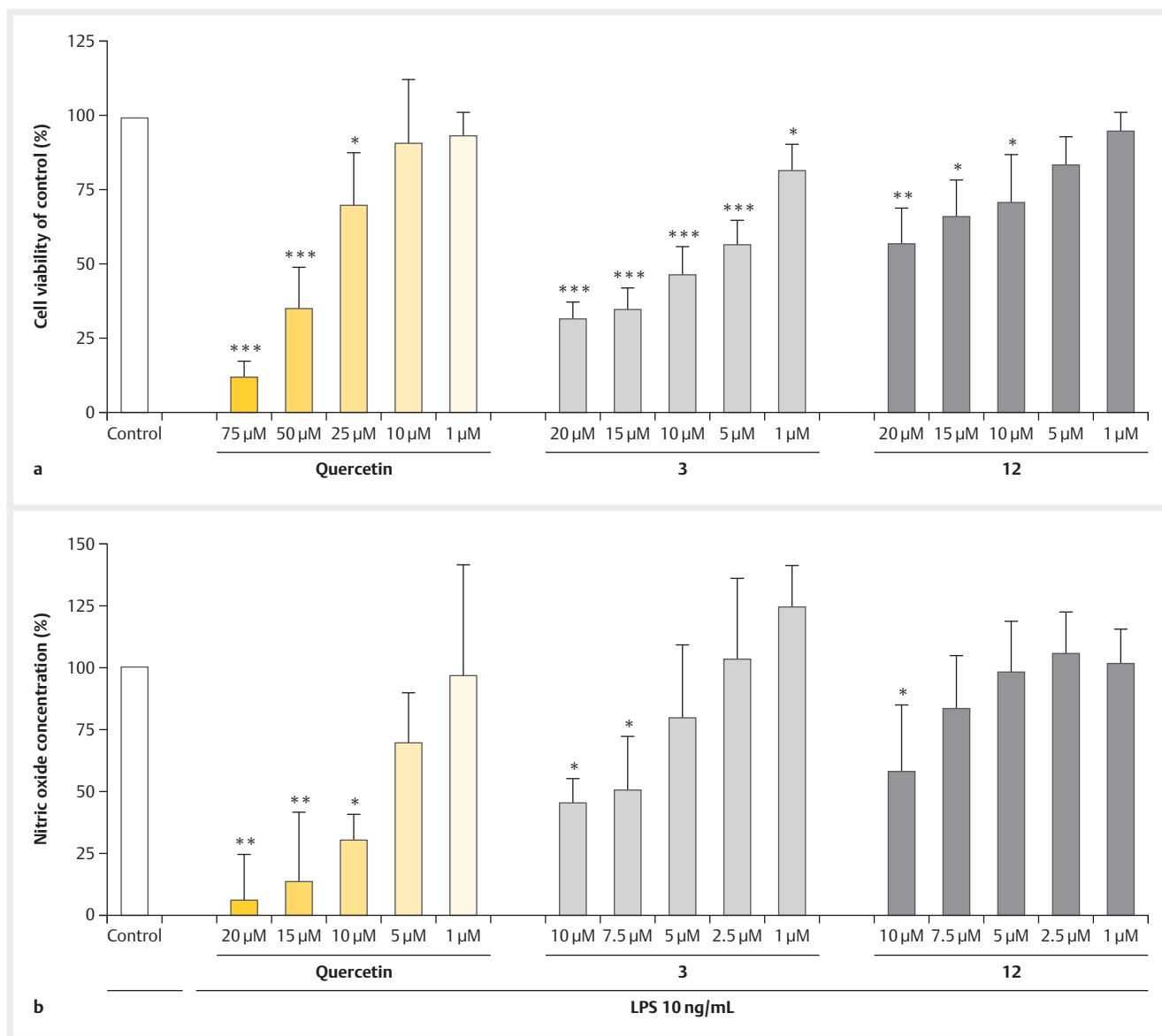
▶ **Fig. 6 a** Viability of RAW 264.7-cells influenced by **3** and **12** (20, 15, 10, 5, and 1 μM) as test compounds and quercetin (75, 50, 25, 10, and 1 μM) as positive control; n = 3 in sextuplicates; mean ± SD; data were subjected to 1-way ANOVA followed Dunnett's post-test using GraphPad Prism 5 software (significance level: $^*p < 0.05$, $^{**}p < 0.01$, $^{***}p < 0.001$); **b** Influence of **3** and **12** (10, 7,5, 5, 2.5, and 1 μM) as test compounds and quercetin (20, 15, 10, 5, and 1 μM) as positive control on NO concentration in the cell supernatant of RAW 264.7 cells stimulated with LPS (10 ng/mL); control (= 100 %): NO concentration in cell supernatant of RAW 264.7 cells stimulated with LPS (10 ng/mL) without substances; n = 3 in pentatupli-cates; mean ± SD; data were subjected to 1-way ANOVA followed by Dunnett's post test using GraphPad Prism 5 software (significance level: $^*p < 0.05$, $^{**}p < 0.01$).

Subfraction PE.2.2 (464 mg, 300–420 mL) was subjected to CPC (flow rate: 5 mL/min, collection: 2 mL/vial, upper phase: satu-rated heptane [3], lower phase: saturated MeCN/MeOH [1 : 1], de-scending mode: 0–1068 mL) to give 4 subfractions (PE.2.2.1–.2.2.4). PE.2.2.4 (45 mg) was separated by preparative HPLC (sys-tem: B, flow rate: 3 mL/min; solvent A: H$_2$O, solvent B: MeCN, gra-dient: 0–5 min 80 % B, 5–7 min 80 % → 85 % B, 7–38 min 85 % B, 38–40 min 85 % → 100 % B, 40–45 min 100 % B, 45–47 min 100 % → 80 % B, 47–50 min 80 % B) to give **15** (4.5 mg, t_R: 27.6 min), **5** (3.4 mg, t_R: 30.0 min), and **16** (6.6 mg, t_R: 34.0 min).

PE.2.3 (764 mg, 420–540 mL) was applied to CPC (flow rate: 5 mL/min, collection 2 mL/vial, upper phase: saturated n-hexane [2], lower phase: saturated MeCN/MeOH [2 : 1], descending mode: 0–1028 mL, ascending mode: 1028–1254 mL) to yield 11 subfractions (PE.2.3.1–.2.3.11).

PE.2.3.2 (357 mg, 94–144 mL) was further fractionated by RP-18 flash chromatography (solvent A: H$_2$O, solvent B: MeCN, flow rate: 5 mL/min, collection: 5 mL/vial, gradient: 0–2 min 40 % B, 2–92 min 40 % → 70 % B, 92–93 min 70 → 98 % B, 93–103 min 98 % B) to provide 7 subfractions (PE.2.3.2.1–2.3.2.7).

PE.2.3.2.2 (10.3 mg, 210–260 mL) was separated by semipreparative HPLC (system: A, flow rate: 3 mL/min, solvent A: H_2O, solvent B: MeCN, gradient: 0–5 min 55% B, 5–7 min 55% → 70% B, 7–32 min 70% B, 32–34 min 70% → 98% B, 34–40 min 98% B, 40–42 min 98% → 55% B, 42–50 min 55% B) to isolate **6** (1.0 mg, t_R: 31.4 min) and **7** (1.5 mg, t_R: 37.0 min).

PE.2.3.2.5 (86 mg, 370–410 mL) was applied to semipreparative HPLC (system: A, flow rate: 3 mL/min, solvent A: H_2O, solvent B: MeCN, gradient: 0–5 min 75% B, 5–7 min 75% → 84% B, 7–32 min 84% B, 32–34 min 84% → 100% B, 34–40 min 100% B, 40–42 min 100% B → 75% B, 42–50 min 75% B) to give **17** (2.4 mg, t_R: 31.9 min) and **5** (15.2 mg, t_R: 35.6 min).

PE.2.3.2.6 (57 mg, 410–470 mL) was separated by semipreparative HPLC (system: A, flow rate: 3 ml/min, solvent A: H_2O, solvent B: MeCN, gradient: 0–5 min 80% B, 5–7 min 80% → 86% B, 7–32 min 86% B, 32–34 min 86% → 100% B, 34–43 min 100% B, 43–45 min 100% → 80% B, 45–50 min 80% B) to yield again **5** (2.4 mg, t_R: 29.9 min).

Hirsutofolin A (**1**): Colorless oil (5.2 mg); $[\alpha]_D^{25}$ + 5.8 (c 0.65, MeOH), ^1H NMR data ($CDCl_3$, 600 MHz) and ^{13}C NMR data ($CDCl_3$, 150 MHz) see ▶ **Table 1**; ESI-HRMS m/z 485.3266 [M + H]$^+$ (calcd. for $C_{30}H_{45}O_5$, 485.3262 [M + H]$^+$).

Peroxyhirsutofolin A (**2**): Colorless oil (6.3 mg); $[\alpha]_D^{25}$ + 12.0 (c 0.79, MeOH), ^1H NMR data ($CDCl_3$, 600 MHz) and ^{13}C NMR data ($CDCl_3$, 150 MHz) see ▶ **Table 1**; ESI-HRMS m/z 501.3220 [M + H]$^+$ (calcd. for $C_{30}H_{45}O_6$, 501.3211 [M + H]$^+$).

Hirsutofolin B (**3**): Colorless oil (34.6 mg); $[\alpha]_D^{25}$ − 12.8 (c 1.15, MeOH), ^1H NMR data ($CDCl_3$, 600 MHz) and ^{13}C NMR data ($CDCl_3$, 150 MHz) see ▶ **Table 1**; ESI-HRMS m/z 499.3424 [M + H]$^+$ (calcd. for $C_{31}H_{47}O_5$, 499.3418 [M + H]$^+$).

3‴-Hydroperoxyisohirsutofolin B (**4**): Colorless oil (4.1 mg); $[\alpha]_D^{25}$ + 20.1 (c 0.52, MeOH), ^1H NMR data ($CDCl_3$, 600 MHz) and ^{13}C NMR data ($CDCl_3$, 150 MHz) see ▶ **Table 1**; ESI-HRMS m/z 553.3139 [M + Na]$^+$ (calcd. for $C_{31}H_{46}O_7Na$, 553.3136 [M + Na]$^+$).

Hirsutuman B (**5**): Colorless oil (26.4 mg); $[\alpha]_D^{25}$ − 61.9 (c 0.68, MeOH), ^1H NMR data ($CDCl_3$, 600 MHz) and ^{13}C NMR data ($CDCl_3$, 150 MHz) see ▶ **Table 2**; ESI-HRMS m/z 499.3426 [M + H]$^+$ (calcd. for $C_{31}H_{47}O_5$, 499.3418 [M + H]$^+$).

3‴-Hydroxyisohirsutuman A (**6**): Colorless oil (1.0 mg); $[\alpha]_D^{25}$ − 35.2 (c 0.13, MeOH), ^1H NMR data ($CDCl_3$, 600 MHz) and ^{13}C NMR data ($CDCl_3$, 150 MHz) see ▶ **Table 2**; ESI-HRMS m/z 501.3214 [M + H]$^+$ (calcd. for $C_{30}H_{45}O_6$, 501.3211 [M + H]$^+$).

3‴-Hydroxyisohirsutuman B (**7**): Colorless oil (6.0 mg); $[\alpha]_D^{25}$ − 69.5 (c 0.19, MeOH), ^1H NMR data ($CDCl_3$, 600 MHz) and ^{13}C NMR data ($CDCl_3$, 150 MHz) see ▶ **Table 2**; ESI-HRMS m/z 515.3364 [M + H]$^+$ (calcd. for $C_{31}H_{47}O_6$, 515.3367 [M + H]$^+$).

Hyperihirsan B (**8**): Colorless oil (1.4 mg); $[\alpha]_D^{25}$ + 47.9 (c 0.18, MeOH), ^1H NMR data ($CDCl_3$, 600 MHz) and ^{13}C NMR data ($CDCl_3$, 150 MHz) see ▶ **Table 3**; ESI-HRMS m/z 531.3310 [M + H]$^+$ (calcd. for $C_{31}H_{47}O_7$, 531.3316 [M + H]$^+$).

Pyranohyperihirsan A (**9**): Colorless oil (2.3 mg); $[\alpha]_D^{25}$ − 24.7 (c 0.29, MeOH), ^1H NMR data ($CDCl_3$, 600 MHz) and ^{13}C NMR data ($CDCl_3$, 150 MHz) see ▶ **Table 3**; ESI-HRMS m/z 517.3169 [M + H]$^+$ (calcd. for $C_{30}H_{45}O_7$, 517.3160 [M + H]$^+$).

Pyranohyperihirsan B (**10**): Colorless oil (2.0 mg); $[\alpha]_D^{25}$ − 30.7 (c 0.25, MeOH), ^1H NMR data ($CDCl_3$, 600 MHz) and ^{13}C NMR data ($CDCl_3$, 150 MHz) see ▶ **Table 3**; ESI-HRMS m/z 531.3319 [M + H]$^+$ (calcd. for $C_{31}H_{47}O_7$, 531.3316 [M + H]$^+$).

Hirsutusal A (**11**): Colorless oil (1.4 mg); $[\alpha]_D^{25}$ + 36.7 (c 0.18, MeOH), ^1H NMR data ($CDCl_3$, 600 MHz) and ^{13}C NMR data ($CDCl_3$, 150 MHz) see ▶ **Table 4**; ESI-HRMS m/z 485.3260 [M + H]$^+$ (calcd. for $C_{30}H_{45}O_5$, 485.3262 [M + H]$^+$).

Hirsutusal B (**12**): Colorless oil (2.0 mg); $[\alpha]_D^{25}$ − 6.9 (c 0.24, MeOH), ^1H NMR data ($CDCl_3$, 600 MHz) and ^{13}C NMR data ($CDCl_3$, 150 MHz) see ▶ **Table 4**; ESI-HRMS m/z 499.3416 [M + H]$^+$ (calcd. for $C_{31}H_{47}O_5$, 499.3418 [M + H]$^+$).

Hirsutusals C and D (**13** and **14**): Colorless oil (2.8 mg); ^1H NMR data ($CDCl_3$, 600 MHz) and ^{13}C NMR data ($CDCl_3$, 150 MHz) see ▶ **Table 4**; ESI-HRMS m/z 499.3420 [M + H]$^+$ (calcd. for $C_{31}H_{47}O_5$, 499.3418 [M + H]$^+$).

Hookerione C (**15**): Colorless oil (4.5 mg); $[\alpha]_D^{25}$ + 6.6 (c 0.56, MeOH), ^1H NMR data ($CDCl_3$, 600 MHz) and ^{13}C NMR data ($CDCl_3$, 150 MHz) see ▶ **Table 5**; ESI-HRMS m/z 483.3110 [M + H]$^+$ (calcd. for $C_{30}H_{43}O_5$, 483.3105 [M + H]$^+$).

Hirsuton A (**16**): Colorless oil (6.1 mg); $[\alpha]_D^{25}$ + 3.7 (c 0.83, MeOH), ^1H NMR data ($CDCl_3$, 600 MHz) and ^{13}C NMR data ($CDCl_3$, 150 MHz) see ▶ **Table 5**; ESI-HRMS m/z 497.3263 [M + H]$^+$ (calcd. for $C_{31}H_{45}O_5$, 497.3262 [M + H]$^+$).

Hirsuton B (**17**): Colorless oil (2.4 mg); $[\alpha]_D^{25}$ + 6.6 (c 0.30, MeOH), ^1H NMR data ($CDCl_3$, 600 MHz) and ^{13}C NMR data ($CDCl_3$, 150 MHz) see ▶ **Table 5**; ESI-HRMS m/z 497.3263 [M + H]$^+$ (calcd. for $C_{31}H_{45}O_5$, 497.3262 [M + H]$^+$).

Hyperihirsolin A (**18**): Colorless oil (5.0 mg); $[\alpha]_D^{25}$ − 25.3 (c 0.62, MeOH), ^1H NMR data ($CDCl_3$, 600 MHz) and ^{13}C NMR data ($CDCl_3$, 150 MHz) see ▶ **Table 6**; ESI-HRMS m/z 523.3036 [M + Na]$^+$ (calcd. for $C_{31}H_{44}O_6Na$, 523.3036 [M + Na]$^+$).

Hyperihirsolin B (**19**): Colorless oil (7.2 mg); $[\alpha]_D^{25}$ − 13.0 (c 0.90, MeOH), ^1H NMR data ($CDCl_3$, 600 MHz) and ^{13}C NMR data ($CDCl_3$, 150 MHz) see ▶ **Table 6**; ESI-HRMS m/z 537.3188 [M + Na]$^+$ (calcd. for $C_{31}H_{46}O_6Na$, 537.3187 [M + Na]$^+$).

Proliferation Assay

For the proliferation assay, an SV-40 T transfected human microvascular HMEC-1 was used [41]. HMEC-1 cells (from E. Ades, F. J. Candal, CDC, and T. Lawley, Emory University) were seeded in 96-well microplates (100 μL, 1.5×10^3 cells/well) in ECGM (endothelial cell growth medium (Pelobiotech GmbH) + 10% FCS + antibiotics + supplements). After 24 h of incubation (New Brunswick Scientific, 37 °C, 5% CO_2, 95% humidity), the medium in a reference plate was removed. These cells were stained with crystal violet solution for 10 min and washed with distilled water serving the baseline. The other plates were treated with either the isolated substances **1–5, 7, 10–12, 15, 16, 18,** and **19** or hyperforin (PhytoLab GmbH & Co. KG) in increasing concentrations (dissolved in DMSO as the stock solution). Batches were incubated for 72 h and stained as previously described. Sodium citrate solution 0.05 M 100 µl (in EtOH 50%) was added, and absorbance was measured with Tecan SpectraFluor Plus at 560 nm. The IC_{50} values ± confidence intervals (in µM) were calculated with GraphPad Prism 5 software (3 independent experiments, each concentration in sextuplicates. Pure solvent (ECGM) was used as a negative control. The effect of the tested concentrations on the viability of HMEC-1 cells was determined after 24 h of incubation using an

MTT assay according to [42] (3 independent experiments in sextuplicates, supporting information exemplarily given for **2, 4,** and **11**).

Purity of tested compounds

The purity of tested compounds was determined by HPLC-DAD analysis using the Max-Plot-option of the HPLC system (EliteLaChrom system with EZChrom Elite 3.1.7 Software, Hitachi) followed by blank subtraction and normalization (Supplementary Information **Figs. 85S–87S**).

ICAM-1 Assay

The ICAM-1-assay was performed in 24-well microplates. Confluent grown HMEC-1 cells were pre-incubated with either the isolated substances **1–5, 7,** and **10–12** (50, 25, 12.5, and 6.25 µM), hyperforin (Phytolab GmbH & Co; 5, 2.5, 1, and 0.5 µM), parthenolide (Calbiochem; 5 µM, positive control), or ECGM (PeloBiotech GmbH) as a negative control. After 30 min, TNF-α (10 ng/mL, Sigma-Aldrich) was added to stimulate the ICAM-1 expression on the surface of the cells. The plates were incubated for 24 h. Subsequently, cells were washed with PBS, removed from the plate with trypsin/EDTA, and fixed with formalin. After adding 5 µL FITC-labelled mouse antibody against ICAM-1 (Bio-Rad Laboratories, Inc.), the batch was incubated for 20 min at room temperature in the dark. The fluorescence intensity was measured by FACS analysis (Becton Dickinson Facscalibur). The ICAM-1-expression of the cells, which were just treated with TNF-α, was set as 100% (maximum ICAM-1-expression). Three independent experiments were performed in duplicates [43].

Griess Assay

RAW 264.7 (ATCC) cells are murine macrophages, which were transfected with the Abelson leukemia virus. The cells were seeded in 96-well microplates (100 µL, 8×10^4 cells/well) in RPMI 1640 medium (Biochrom GmbH) + 10% FCS + 1% glutamine. After 24 h incubation, the substances to be tested (**3** and **12**) were added in a concentration range of 1–10 µM. Quercetin was used as a positive control (1–20 µM). Contemporary NO production of the macrophages was stimulated with lipopolysaccharide (LPS, Sigma-Aldrich, 10 ng/mL). After incubation for 24 h, supernatants were mixed one-to-one with Griess reagent (1% sulfanilamide, Sigma Aldrich + 0.1% naphthylethylendiamine dihydrochloride, Sigma Aldrich + 0.35% H_3PO_4 in water). This batch was stored at room temperature in the dark for 15 min, and absorbance was measured with Tecan SpectraFluor Plus at 560 nm. The nitrite concentration was calculated from a standard curve generated with $NaNO_2$. Three independent experiments were performed in pentaplicates.

To study cytotoxic effects, compounds **3** and **12** were investigated regarding their influence on the viability of RAW 264.7 cells (1–20 µM) after 24 h of incubation using an MTT assay according to [42] (3 independent experiments in sextuplicates). Quercetin was used as a positive control (1–75 µM).

Supporting information

Supporting Information includes the following: 1D and 2D NMR spectra of compounds **1–19** (**Figs. 4S–8S, 10S–78S, 80S, 81S**); indicatives and principal structure elucidation strategy of a PPAP based on adamantane and homoadamantane core and substituents (**Figs. 1S–3S**); CD spectra of isolated compounds in MeOH (**Figs. 82S–84S**); purity determination of isolated compounds with HPLC (**Figs. 85S–87S**); **Figs. 9S** and **79S**: 3D models of hypothetic H-6α epimer of **1** and compound **18** calculated by ChemBioDraw Ultra 14.0.0.117; the influence of **2, 4,** and **11** on cell viability of HMEC-1 cells (**Fig. 88S**); data of proliferation assay of **1–5, 7, 10–12, 15, 16, 18, 9,** and hyperforin (**Fig. 89S**); and inhibition of TNF-α induced ICAM-1 expression in HMEC-1 cells by **1, 2, 4, 11,** and hyperforin (**Fig. 90S**)

Contributors' Statement

Concept and design of the work: J. Heilmann; data collection: J. Max; analysis and interpretation of the data: J. Heilmann, J. Max; drafting the manuscript: J. Max; critical revision of the manuscript: J. Heilmann.

Conflict of Interest

The authors declare that they have no conflict of interest.

References

[1] Kadereit JW, Kubitzki K. Flowering Plants, Dicotyledons: Lamiales (except Acanthaceae including Avicenniaceae). Berlin: Springer; 2004

[2] Crockett SL, Robson NKB. Taxonomy and chemotaxonomy of the Genus *Hypericum*. Med Aromat Plant Sci Biotechnol 2011; 5: 1–13

[3] Avato P. A Survey on the *Hypericum* Genus: Secondary Metabolites and Bioactivity. In: Atta-ur-Rahman, ed. Studies in natural Products Chemistry: Bioactive natural Products (Part K), Vol. 30. Amsterdam: Elsevier; 2005: 603–634

[4] Crockett SL, Wenzig, EM, Kunert O, Bauer R. Anti-inflammatory phloroglucinol derivatives from *Hypericum empetrifolium*. Phytochem Lett 2008; 1: 37–43

[5] Heilmann J, Winkelmann K, Sticher O. Studies on the antioxidative activity of phloroglucinol derivatives isolated from *Hypericum* species. Planta Med 2003; 69: 202–206

[6] Piccinelli AL, Cuesta-Rubio O, Chica MB, Mahmood N, Pagano B, Pavone M, Barone V, Rastrelli L. Structural revision of clusianone and 7-epi-clusianone and anti-HIV activity of polyisoprenylated benzophenones. Tetrahedron 2005; 61: 8206–8211

[7] Rouger C, Pagie S, Derbré S, Le Ray AM, Richomme P, Charreau B. Prenylated polyphenols from Clusiaceae and Calophyllaceae with immunomodulatory activity on endothelial cells. PLoS One 2016; 11: e0167361

[8] Schmidt S, Jürgenliemk G, Skaltsa H, Heilmann J. Phloroglucinol derivatives from *Hypericum empetrifolium* with antiproliferative activity on endothelial cells. Phytochemistry 2012; 77: 218–225

[9] Stolz ED, Hasse DR, von Poser GL, Rates SMK. Uliginosin B, a natural phloroglucinol derivative, presents a multimediated antinociceptive effect in mice. J Pharm Pharmacol 2014; 66: 1774–1785

[10] Tanaka N, Kubota T, Ishiyama H, Araki A, Kashiwada Y, Takaishi Y, Mikami Y, Kobayashi J. Petiolins A–C, phloroglucinol derivatives from *Hypericum pseudopetiolatum* var. *kiusianum*. Bioorg Med Chem 2008; 16: 5619–5623

[11] Dakanali M, Theodorakis EA. Polyprenylated Phloroglucinols and Xanthones. In: Poupon E, ed. Biomimetic organic Synthesis, Vol. 163. Weinheim: Wiley-VCH; 2011: 433–467

[12] Trifunović S, Vajs V, Macura S, Juranić N, Djarmati Z, Jankov R, Milosavljević S. Oxidation products of hyperforin from *Hypericum perforatum*. Phytochemistry 1998; 49: 1305–1310

[13] Hu LH, Sim KY. Cytotoxic polyprenylated benzoylphloroglucinol derivatives with an unusual adamantyl skeleton from *Hypericum sampsonii* (Guttiferae). Org Lett 1999; 1: 879–882

[14] Hu LH, Sim KY. Complex caged polyisoprenylated benzophenone derivatives, sampsoniones A and B, from *Hypericum sampsonii*. Tetrahedron Lett 1998; 39: 7999–8002

[15] Winkelmann K, Heilmann J, Zerbe O, Rali T, Sticher O. Further prenylated bi- and tricyclic phloroglucinol derivatives from *Hypericum papuanum*. Helv Chim Acta 2001; 84: 3380–3392

[16] Winkelmann K, Heilmann J, Zerbe O, Rali T, Sticher O. New prenylated bi- and tricyclic phloroglucinol derivatives from *Hypericum papuanum*. J Nat Prod 2001; 64: 701–706

[17] Wu CC, Yen MH, Yang SC, Lin CN. Phloroglucinols with antioxidant activity and xanthonolignoids from the heartwood of *Hypericum geminiflorum*. J Nat Prod 2008; 71: 1027–1031

[18] Robson NKB. Studies in the genus *Hypericum* L (Hypericaceae). Sections 17. *Hirtella* to 19. *Coridium*. Phytotaxa 2010; 4: 127–258

[19] Smelcerovic A, Spiteller M. Phytochemical analysis of nine *Hypericum* L. species from Serbia and the FYR Macedonia. Pharmazie 2006; 61: 251–252

[20] Crockett S, Kunert O, Jacob M, Bauer R, Nedialkov P. Antimicrobial acylphloroglucinol derivatives from *Hypericum linarioides* (Hypericaceae). Planta Med 2010; 76: P430

[21] Ishida Y, Shirota O, Sekita S, Someya K, Tokita F, Nakane T, Kuroyanagi M. Polyprenylated benzoylphloroglucinol-type derivatives including novel cage compounds from *Hypericum erectum*. Chem Pharm Bull 2010; 58: 336–343

[22] Zhu HC, Chen CM, Zhang JW, Guo Y, Tan DD, Wei GZ, Yang J, Wang JP, Luo ZW, Xue YB, Zhang YH. Hyperisampsins N and O, two new benzoylated phloroglucinol derivatives from *Hypericum sampsonii*. Chin Chem Lett 2017; 28: 986–990

[23] Yang XW, Wang H, Ma WG, Xia F, Xu G. Homo-adamantane type polyprenylated acylphloroglucinols from *Hypericum pseudohenryi*. Tetrahedron 2017; 73: 566–570

[24] Cruz FG, Teixeira JSR. Polyprenylated benzophenones with a tricyclo [4.3.1.1(3, 8)]undecane skeleton from *Clusia obdeltifolia*. J Braz Chem Soc 2004; 15: 504–508

[25] Xiao ZY, Zeng YH, Mu Q, Shiu WKP, Gibbons S. Prenylated benzophenone peroxide derivatives from *Hypericum sampsonii*. Chem Biodivers 2010; 7: 953–958

[26] Christian OE, Henry GE, Jacobs H, McLean S, Reynolds WF. Prenylated benzophenone derivatives from *Clusia havetiodes* var. *stenocarpa*. J Nat Prod 2001; 64: 23–25

[27] Yang XW, Li MM, Liu X, Ferreira D, Ding Y, Zhang JJ, Liao Y, Qin HB, Xu G. Polycyclic polyprenylated acylphloroglucinol congeners possessing diverse structures from *Hypericum henryi*. J Nat Prod 2015; 78: 885–895

[28] Henry GE, Jacobs H, Carrington CMS, McLean S, Reynolds WF. Prenylated benzophenone derivatives from Caribbean *Clusia* species (Guttiferae). Plukenetiones B–G and xerophenone A. Tetrahedron 1999; 55: 1581–1596

[29] Li D, Xue Y, Zhu H, Li Y, Sun B, Liu J, Yao G, Zhang J, Du G, Zhang Y. Hyperattenins A–I, bioactive polyprenylated acylphloroglucinols from *Hypericum attenuatum* Choisy. RSC Adv 2015; 5: 5277–5287

[30] Hu LH, Sim KY. Sampsoniones C–H, a unique family of polyprenylated benzophenone derivatives with the novel tetracyclo[7.3.1.13, 11.03, 7] tetradecane-2,12,14-trione skeleton, from *Hypericum sampsonii* (Guttiferae). Tetrahedron Lett 1999; 40: 759–762

[31] Liu X, Yang XW, Chen CQ, Wu CY, Zhang JJ, Ma JZ, Wang H, Zhao QS, Yang LX, Xu G. Hypercohones A–C, acylphloroglucinol derivatives with homo-adamantane cores from *Hypericum cohaerens*. Nat Prod Bioprospect 2013; 3: 233–237

[32] Zhou ZB, Zhang YM, Pan K, Luo JG, Kong LY. Cytotoxic polycyclic polyprenylated acylphloroglucinols from *Hypericum attenuatum*. Fitoterapia 2014; 95: 1–7

[33] Ye Y, Yang XW, Xu G. Unusual adamantane type polyprenylated acylphloroglucinols with an oxirane unit and their structural transformation from *Hypericum hookerianum*. Tetrahedron 2016; 72: 3057–3062

[34] Zhu H, Chen C, Yang J, Li XN, Liu J, Sun B, Huang SX, Li D, Yao G, Luo Z, Li Y, Zhang J, Xue Y, Zhang Y. Bioactive acylphloroglucinols with adamantyl skeleton from *Hypericum sampsonii*. Org Lett 2014; 16: 6322–6325

[35] Wang K, Wang YY, Gao X, Chen XQ, Peng LY, Li Y, Xu G, Zhao QS. Polycyclic polyprenylated acylphloroglucinols and cytotoxic constituents of *Hypericum androsaemum*. Chem Biodivers 2012; 9: 1213–1220

[36] Rezanka T, Sigler K. Sinaicinone, a complex adamantanyl derivative from *Hypericum sinaicum*. Phytochemistry 2007; 68: 1272–1276

[37] Tanaka N, Takaishi Y, Shikishima Y, Nakanishi Y, Bastow K, Lee KH, Honda G, Ito M, Takeda Y, Kodzhimatov OK, Ashurmetov O. Prenylated benzophenones and xanthones from *Hypericum scabrum*. J Nat Prod 2004; 67: 1870–1875

[38] Chen JJ, Chen, HJ, Lin YL. Novel polyprenylated phloroglucinols from *Hypericum sampsonii*. Molecules 2014; 19: 19836–19844

[39] Christian OE, McLean S, Reynolds WF, Jacobs H. Prenylated benzophenones from *Hypericum hypericoides*. Nat Prod Com 2008; 3: 1781–1786

[40] Martínez-Poveda B, Verotta L, Bombardelli E, Quesada AR, Medina MÁ. Tetrahydrohyperforin and octahydrohyperforin are two new potent inhibitors of angiogenesis. PLoS One 2010; 5: e9558

[41] Ades EW, Candal FJ, Swerlick RA, George VG, Summers S, Bosse DC, Lawley TJ. 1992. HMEC-1: Establishment of an immortalized human microvascular endothelial cell line. J Invest Dermatol 1992; 99: 683–690

[42] Mosmann T. Rapid colorimetric assay for cellular growth and survival: application to proliferation and cytotoxicity assays. J Immunol Methods 1983; 65: 55–63

[43] Flemming M, Kraus B, Rascle A, Jürgenliemk G, Fuchs S, Fürst R, Heilmann J. Revisited anti-inflammatory activity of matricine *in vitro*: comparison with chamazulene. Fitoterapia 2015; 106: 122–128